Clinical & Translational Immunology

Australian and New Zealand Society for Immunology Inc.

*Clinical & Translational Immunology* 2020; e1213. doi: 10.1002/cti2.1213
www.wileyonlinelibrary.com/journal/cti

ORIGINAL ARTICLE

# *Porphyromonas gingivalis* and *Lactobacillus rhamnosus* GG regulate the Th17/Treg balance in colitis via TLR4 and TLR2

Lu Jia[1], Ruiqing Wu[2], Nannan Han[1], Jingfei Fu[1], Zhenhua Luo[1], Lijia Guo[3], Yingying Su[2], Juan Du[1] & Yi Liu[1]

[1]Laboratory of Tissue Regeneration and Immunology and Department of Periodontics, Beijing Key Laboratory of Tooth Regeneration and Function Reconstruction, School of Stomatology, Capital Medical University, Beijing, China
[2]Beijing Tiantan Hospital, Capital Medical University, Beijing, China
[3]Department of Orthodontics, School of Stomatology, Capital Medical University, Beijing, China

**Correspondence**
Y Liu, Laboratory of Tissue Regeneration and Immunology and Department of Periodontics, Beijing Key Laboratory of Tooth Regeneration and Function Reconstruction, School of Stomatology, Capital Medical University, Beijing, China.
E-mail: lililiuyi@163.com

Received 15 September 2019;
Revised 13 March, 8 September and 21 October 2020;
Accepted 21 October 2020

doi: 10.1002/cti2.1213

*Clinical & Translational Immunology* 2020; **9**: e1213

## Abstract

**Objectives.** $CD4^+$ T cells are the key to many immune–inflammatory diseases mediated by microbial disorders, especially inflammatory bowel disease (IBD). The purpose of this study was to explore how pathogenic and probiotic bacteria directly affect the T helper (Th)17 and T regulatory (Treg) cell balance among $CD4^+$ T cells to regulate inflammation. **Methods.** *Porphyromonas gingivalis* (Pg; ATCC 33277) and *Lactobacillus rhamnosus* GG (LGG; CICC 6141) were selected as representative pathogenic and probiotic bacteria, respectively. Bacterial extracts were obtained via ultrasonication and ultracentrifugation. Flow cytometry, RT-qPCR, ELISAs, immunofluorescence and a Quantibody cytokine array were used. The dextran sodium sulphate (DSS)-induced colitis model was selected for verification. **Results.** The Pg ultrasonicate induced the apoptosis of $CD4^+$ T cells and upregulated the expression of the Th17-associated transcription factor RoR$\gamma$t and the production of the proinflammatory cytokines IL-17 and IL-6, but downregulated the expression of the essential Treg transcription factor Foxp3 and the production of the anti-inflammatory factors TGF-$\beta$ and IL-10 via the TLR4 pathway. However, LGG extract maintained Th17/Treg homeostasis by decreasing the IL-$17^+$ Th17 proportion and increasing the $CD25^+$ $Foxp3^+$ Treg proportion via the TLR2 pathway. *In vivo,* Pg-stimulated $CD4^+$ T cells aggravated DSS-induced colitis by increasing the Th17/Treg ratio in the colon and lamina propria lymphocytes (LPLs), and Pg + LGG-stimulated $CD4^+$ T cells relieved colitis by decreasing the Th17/Treg ratio via the JAK-STAT signalling pathway. **Conclusions.** Our findings suggest that pathogenic Pg and probiotic LGG can directly regulate the Th17/Treg balance via different TLRs.

**Keywords:** *Porphyromonas gingivalis*, *Lactobacillus rhamnosus* GG, colitis, Th17, Treg, toll-like receptor

## INTRODUCTION

Microbial dysbiosis is a state of imbalance in the relative richness or influence of species within disease-related microbial communities and is a potential trigger for mucosal inflammatory diseases, including inflammatory bowel disease (IBD) and periodontitis.[1] As microbial imbalance is an initiating factor for these diseases, their progression is primarily regulated by the interactions between microorganisms and host immune responses. Consequently, how microbes communicate with hosts in the development of local and distant inflammation has recently become a hot spot in the study of pathogenesis.[2] Herein, we show that $CD4^+$ T helper (Th) cells play a pivotal role in maintaining immune homeostasis in this process, among which the balance between proinflammatory $CD4^+$ IL-$17^+$ Th17 cells and immunosuppressive $CD4^+$ $CD25^+$ $Foxp3^+$ T regulatory (Treg) cells is proven to be the cornerstone. Th17 cells exhibit dual characteristics in the pathogenesis of colitis.

On the one hand, excessive activation of IL-$17^+$ Th17 cells aggravates colitis.[3] Colitis can be induced by transferring well-differentiated Th17 cells to mice lacking immune cells.[4] On the other hand, IL-17 deficiency does not prevent colitis mediated by transplantation of $CD4^+$ T cells without Treg cells, and the lack of IL-17 receptor signalling in pathogenic Th1 cells can aggravate colitis.[5] Besides, a lack of Tregs in gut-associated lymphoid tissue (GALT) or an inability to circulate naturally to the inflammation site results in an immune response to the symbiotic flora and subsequent colitis.[6] Moreover, compared with healthy subjects, a higher Th17-to-Treg cell ratio accompanied by a significantly proinflammatory cytokine microenvironment was detected in peripheral blood samples from IBD patients.[7] In general, it is essential to understand how the Th17/Treg cell equilibrium regulates inflammatory progression under different pathological conditions because it may be a therapeutic target for mucosal inflammatory diseases.

Periodontitis is a common infectious disease of the mouth and is characterised by the destruction of the periodontal supporting tissue and ultimate tooth loss. Also, periodontitis has been confirmed to be closely associated with various systemic diseases, such as cardiovascular and cerebrovascular diseases, diabetes, rheumatoid arthritis[8] and even Alzheimer's disease.[9] *Porphyromonas gingivalis* (*P. gingivalis,* Pg) is one of the main pathogenic bacteria in periodontitis (and the most studied) and is often selected as a representative bacterial strain to study the pathogenesis of inflammation.[10] Although the representative cytokines and markers of Th1, Th2, Th17 and Treg cells have been described in the pathogenesis of periodontitis based on Pg as a model,[11] it is not clear whether Pg directly mediates the change in Th17/Treg balance during inflammation occurrence and development.

As a result of the slow research progress in identifying new antibiotics and the increase in drug-resistant pathogens, probiotics have focused on treating mucosal inflammatory diseases. The most common probiotics, including *Lactobacillus* and *Bifidobacterium*, possess antibacterial and antifungal activity[12] and have the function of maintaining mucosal and immune system homeostasis.[13] Recent studies have confirmed the positive role the probiotic *Lactobacillus* plays in preventing and treating oral and gastrointestinal diseases.[14] For instance, new randomised clinical trials (RCTs) have shown that the supplemental application of *Lactobacillus reuteri* for chronic periodontitis treatment can effectively control gingival inflammation and reduce periodontal pocket depth.[15] The probiotic *Lactobacillus paracasei* LS2 can ameliorate the symptoms of dextran sodium sulphate (DSS)-induced colitis by increasing the proportion of IL-$10^+$ $Foxp3^+$ Treg cells among colonic lamina propria lymphocytes (LPLs).[16] We previously found that after initial periodontal treatment, the proportion of *Lactobacillus* in the periodontal microenvironment increased, whereas the ratio of Pg decreased.[17] However, it is not clear whether *Lactobacillus* can improve inflammation by affecting the Th17/Treg balance.

Maintaining the balance between pathogens and the host via Toll-like receptors (TLRs) is one of the most critical ways by which probiotics can play a beneficial role.[18] TLRs are pathogen-associated molecular pattern (PAMP)-recognition receptors shown to be expressed not only on the surface of innate immune cells and specialised antigen-presenting cells (APCs) but also on the surface of $CD4^+$ T cells.[19] TLR signalling has been confirmed to affect the function and proliferation of Treg cells directly. This proliferation response is triggered by T-cell receptors (TCRs) and stimulated by IL-2, with no need for APCs.[20] Furthermore, in addition to TLRs, studies have shown that the proinflammatory cytokine environment and

specific transcription factors are indispensable for regulating the Th17/Treg balance.[21] Many Foxp3$^+$ T cells in the intestinal tract express a large amount of RoR$\gamma$t (a key transcription factor for Th17 differentiation) and produce IL-17. Furthermore, more than a quarter of IL-17$^+$ T cells express Foxp3 (an essential transcription factor for Treg differentiation) at a certain stage in their development.[22] These findings powerfully illustrate the close relationship between Treg and Th17 cells and suggest that their mutual induction may be a specific microbial immune response strategy.

This study aimed to explore whether and how the pathogenic Pg (ATCC 33277) and the probiotic *L. rhamnosus* GG (LGG; CICC 6141) directly regulate the Th17/Treg balance in the CD4$^+$ T-cell system by regulating TLRs, proinflammatory cytokines and critical transcription factors. We found that the pathogenic Pg ultrasonicate increased the IL-17$^+$ Th17 cell proportion and decreased the CD25$^+$ Foxp3$^+$ Treg cell proportion through the TLR4-mediated signalling pathway, resulting in a disequilibrium between the frequency and function of related cytokines (IL-17, IL-6, TGF-$\beta$ and IL-10) and transcription factors (RoR$\gamma$t and Foxp3). Nevertheless, probiotic LGG ultrasonicate reduced the proportion of Th17 cells and increased Treg cells' proportion via the TLR2 signalling pathway to restore the Th17/Treg balance and maintain the immunomodulatory effect of CD4$^+$ T cells. This discovery provides a new theoretical basis for applying microbial therapy for dysbacteriosis and inflammation-related diseases and is of great significance for developing effective immunological responses to CD4$^+$ T-cell-mediated intestinal inflammation.

## RESULTS

### LGG ultrasonicate weakened the proapoptotic effect of Pg ultrasonicate on activated CD4$^+$ T cells

To detect the effects of Pg or LGG ultrasonicate on the cell proliferation and apoptosis of activated CD4$^+$ T cells, we used flow cytometry as the following groups: (1) control group without bacterial ultrasonicate; (2) 25 $\mu$g mL$^{-1}$ Pg or LGG ultrasonicate group; (3) 50 $\mu$g mL$^{-1}$ Pg or LGG ultrasonicate group; and (4) 100 $\mu$g mL$^{-1}$ Pg or LGG ultrasonicate group. We found that Pg extract promoted activated CD4$^+$ T-cell apoptosis in a concentration-dependent manner, while LGG ultrasonicate promoted cell proliferation, and 50 $\mu$g mL$^{-1}$ was the lowest effective concentration for Pg or LGG ultrasonicate (detailed in Supplementary figure 1). Then, equal amounts of 50 $\mu$g mL$^{-1}$ Pg and LGG extract were added to the medium to observe the biological effects of a balanced pathogenic and probiotic bacteria presence. The cellular proliferation index in the balanced Pg + LGG group was significantly higher than that in the Pg group (Figure 1a and b, $P < 0.05$, Pg + LGG group *versus* Pg-50 group; 22.8 $\pm$ 1.9 *versus* 18.0 $\pm$ 1.8), while the late apoptosis rate in the Pg + LGG group was significantly lower than that in the Pg group (Figure 1c and d, $P < 0.001$, Pg + LGG group *versus* Pg-50 group; 8.2% $\pm$ 0.1% *versus* 12.6% $\pm$ 0.2%). These results suggest that although LGG ultrasonicate alone does not lead to an apparent change in the apoptosis of activated CD4$^+$ T cells (Supplementary figure 1), it does significantly weaken the proapoptotic effect of Pg ultrasonicate when coadministered. The weakening effect of LGG on the apoptosis induced by Pg was also manifested in inactive CD4$^+$ T cells (detailed in Supplementary figures 2 and 3).

### Pg ultrasonicate increased the percentage of Th17 cells and decreased the proportion of Treg cells, which was reversed by neutralisation with LGG ultrasonicate

Pg, LGG or Pg + LGG mixed ultrasonicate at a concentration of 50 $\mu$g mL$^{-1}$ was added to the cultures to detect different microbial extracts' effect on the Th17/Treg balance among activated CD4$^+$ T cells. The addition of Pg extract significantly increased the percentage of IL-17$^+$ Th17 cells among the total CD4$^+$ T cells (Figure 1e and f, $P < 0.001$). However, the proportion of Th17 cells in the Pg + LGG mixed ultrasonicate group was significantly lower than that in the Pg group ($P < 0.001$, Pg + LGG group *versus* Pg-50 group; 15.4% $\pm$ 1.4% *versus* 23.6% $\pm$ 1.6%), which suggests that a balance between LGG and Pg is beneficial to reduce the high IL-17 expression in CD4$^+$ T cells caused by the pathogenic Pg ultrasonicate. Notably, there was no significant difference in the proportion of Th17 cells in the single LGG group than the control group ($P > 0.05$).

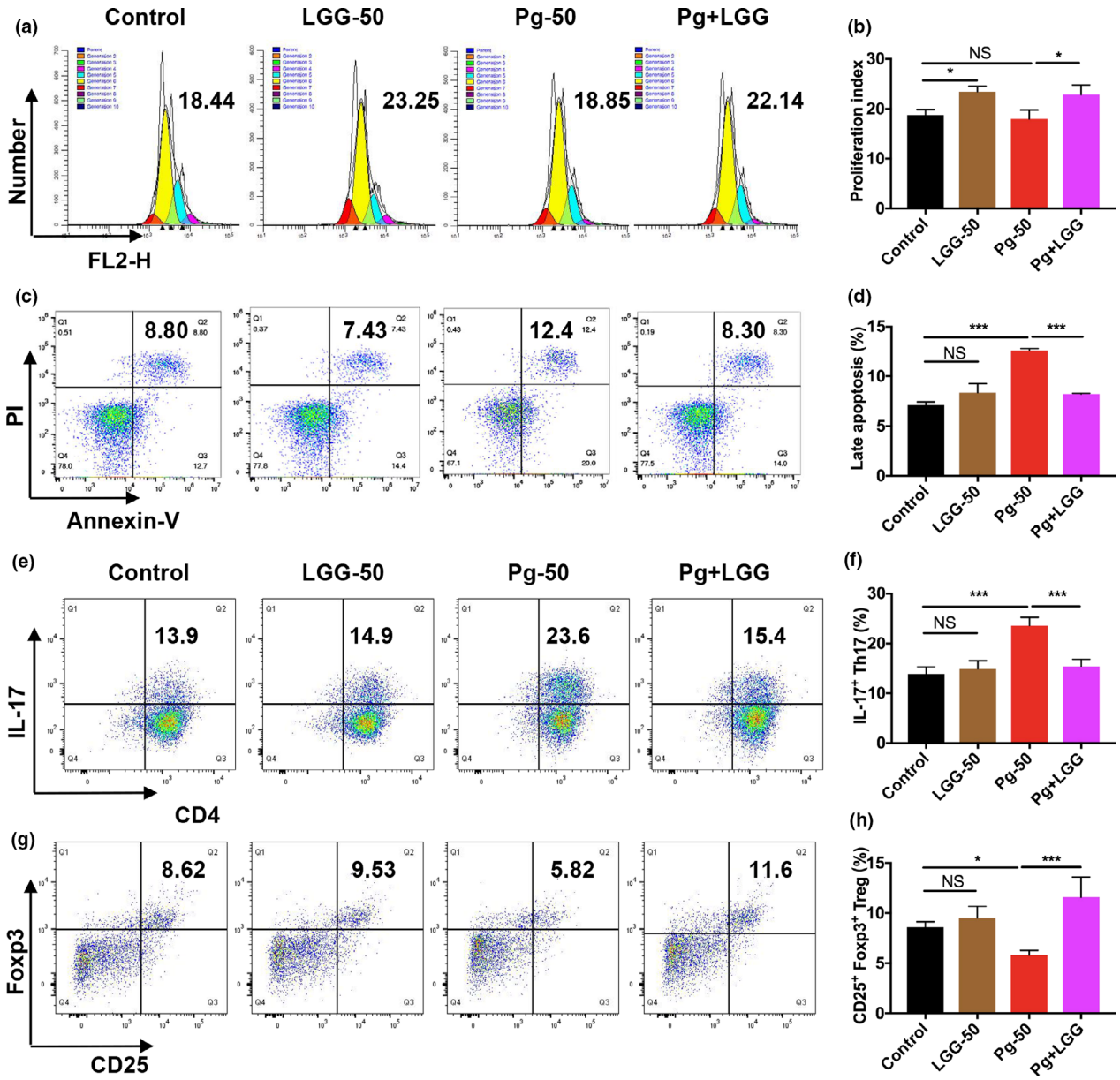


**Figure 1.** LGG ultrasonicate reverses the proapoptotic effect and Th17/Treg imbalance induced by Pg extract in activated $CD4^+$ T cells. Primary $CD4^+$ T cells were activated by anti-CD3 and anti-CD28 antibodies, and a 50 μg $mL^{-1}$ final concentration of LGG or Pg ultrasonicate alone or in combination (Pg + LGG) was added to the culture medium for 48 h prior to detection of cell proliferation and apoptosis and the proportion of Th17 and Treg cells in the system. Th17 cells were characterised as $CD4^+$ $IL\text{-}17^+$ cells, and Treg cells were characterised as $CD4^+$ $CD25^+$ $Foxp3^+$ cells. **(a)** Peak patterns were detected via flow cytometry after CFSE labelling, and **(b)** cell proliferation in each group was analysed. **(c)** Late apoptosis rate represented by Annexin V and PI double-positive staining and the statistical analysis **(d)**. **(e, f)** The proportion of $CD4^+$ $IL\text{-}17^+$ Th17 cells and **(g, h)** the percentage of $CD4^+$ $CD25^+$ $Foxp3^+$ Treg cells among the total $CD4^+$ T cells in each group were detected via flow cytometry and statistically analysed. The data represent three repeated independent experiments and are shown as the mean ± SD (Bonferroni's multiple comparisons test; $*P < 0.05$; $***P < 0.001$; NS, no significant difference).

In terms of Treg percentage changes, the proportion of $CD25^+$ $Foxp3^+$ cells among the total $CD4^+$ T cells was reduced by Pg ultrasonicate challenge (Figure 1g and h, $P < 0.05$). However, the Pg-LGG mixed ultrasonicate group had a greater proportion of Tregs than the Pg group ($P < 0.001$, Pg + LGG group *versus* Pg-50 group; 11.6% ± 2.0% *versus* 5.8% ± 0.5%). Compared

with the control group, the LGG group did not significantly increase the Treg percentage ($P > 0.05$). By calculating the ratio of Th17 cells to Treg cells, a large increase in the Th17/Treg ratio was found in the Pg extract-stimulated group (Supplementary figure 4a, $P < 0.01$). Nevertheless, the Th17/Treg ratio in the Pg-LGG group was significantly reduced compared with that in the Pg group ($P < 0.001$).

Collectively, these results show that LGG alleviates the Pg-induced proinflammatory effect on $CD4^+$ T cells by reducing the Th17 proportion and increasing the Treg proportion to maintain the stability of the Th17/Treg balance. This conclusion was further confirmed by results that the expression of representative Th17 cytokines (IL-17 and IL-6) was significantly downregulated, and the expression of Treg-related cytokines (TGF-β and IL-10) was markedly upregulated at the transcription and secretion levels by LGG ultrasonicate-neutralised Pg extract treatment (Supplementary figure 4).

## Pg ultrasonicate upregulated the Th17/Treg ratio via the TLR4 pathway

We detected the expression levels of cytokines (IL-17, IL-6, TGF-β and IL-10) and transcription factors (RoRγt and Foxp3) by a TLR blocking assay to explore the roles that TLR2 and TLR4 play in mediating the increase in the Th17/Treg ratio during $CD4^+$ T-cell stimulation with Pg ultrasonicate.

For TLR4, the transcription levels of RoRγt, IL-17 and IL-6 in the Pg + anti-TLR4 group were significantly lower than those in the Pg group (Figure 2a and e, IL-17: $P < 0.01$; IL-6: $P < 0.05$; RoRγt: $P < 0.01$), together with a marked decrease in protein secretion (Figure 2c, IL-17: $P < 0.001$; IL-6: $P < 0.01$). However, the gene expression of Foxp3, TGF-β and IL-10 in the Pg + anti-TLR4 group was higher than that of those in the Pg group (Figure 2b and e, TGF-β: $P < 0.01$; IL-10: $P < 0.001$; Foxp3: $P < 0.01$), and the concentration of secreted TGF-β and IL-10 was markedly increased accordingly (Figure 2d, TGF-β: $P < 0.001$; IL-10: $P < 0.01$). These results consistently indicate that the pathogenic Pg extract promotes Th17 cell development and inhibits Treg formation through TLR4 recognition on the surface of activated $CD4^+$ T cells (a schematic diagram of the pathway is shown in Figure 2f).

For TLR2, the expression of RoRγt, IL-17 and IL-6 in the Pg + anti-TLR2 group was significantly higher than that of those in the Pg group (RoRγt: $P < 0.001$; IL-17: $P < 0.001$; IL-6: $P < 0.01$), and the production of IL-17 and IL-6 in the culture supernatants in the Pg + anti-TLR2 group was higher than that of those in the Pg group (IL-17: $P < 0.01$; IL-6: $P < 0.01$). The TGF-β and IL-10 levels in the Pg + anti-TLR2 group were significantly lower than those in the Pg group (TGF-β: $P < 0.01$; IL-10: $P < 0.05$), along with reduced Foxp3 gene expression ($P < 0.05$). Collectively, these results indicate that blockade of TLR2 increases the proportion of Th17 cells and decreases the proportion of Treg cells. In other words, activating TLR2 triggers a decrease in the Th17/Treg cell ratio.

## LGG ultrasonicate decreased the Th17/Treg ratio via the TLR2 pathway when Pg ultrasonicate disrupted the balance

Considering the previous finding that Pg + LGG extract overturns the increase in the Th17/Treg ratio caused by Pg ultrasonicate, we hypothesised that the LGG ultrasonicate reduces the Th17 proportion and increases the Treg proportion through activation of TLR2. We added a TLR4 or TLR2 antagonist to the system of activated $CD4^+$ T cells stimulated with Pg + LGG ultrasonicate. We found that the expression of RoRγt in the Pg + LGG + anti-TLR2 group was markedly greater than that in the Pg + LGG group (Figure 3e, $P < 0.001$). In addition, the production of IL-17 and IL-6 by Th17 cells in the Pg + LGG + anti-TLR2 group was remarkably greater than that of those in the Pg + LGG group (Figure 3c, IL-17: $P < 0.01$; IL-6: $P < 0.01$). Moreover, the expression of Foxp3 in the Pg + LGG + anti-TLR2 group was distinctly lower than that in the Pg + LGG group ($P < 0.001$). The content of TGF-β and IL-10 in the Pg + LGG + anti-TLR2 group was markedly lower than that of those in the Pg + LGG group (Figure 3d, TGF-β: $P < 0.01$; IL-10: $P < 0.01$) and was as low as that in the Pg group ($P > 0.05$). These results suggest that blocking the TLR2-mediated pathway in the Pg + LGG-stimulated $CD4^+$ T cells restores the increase in RoRγt, IL-17 and IL-6 expression and the decrease in Foxp3, TGF-β and IL-10 production. Flow cytometry analyses showing the percentages of $IL\text{-}17^+$ Th17 cells and $CD25^+$ $Foxp3^+$ Tregs in the

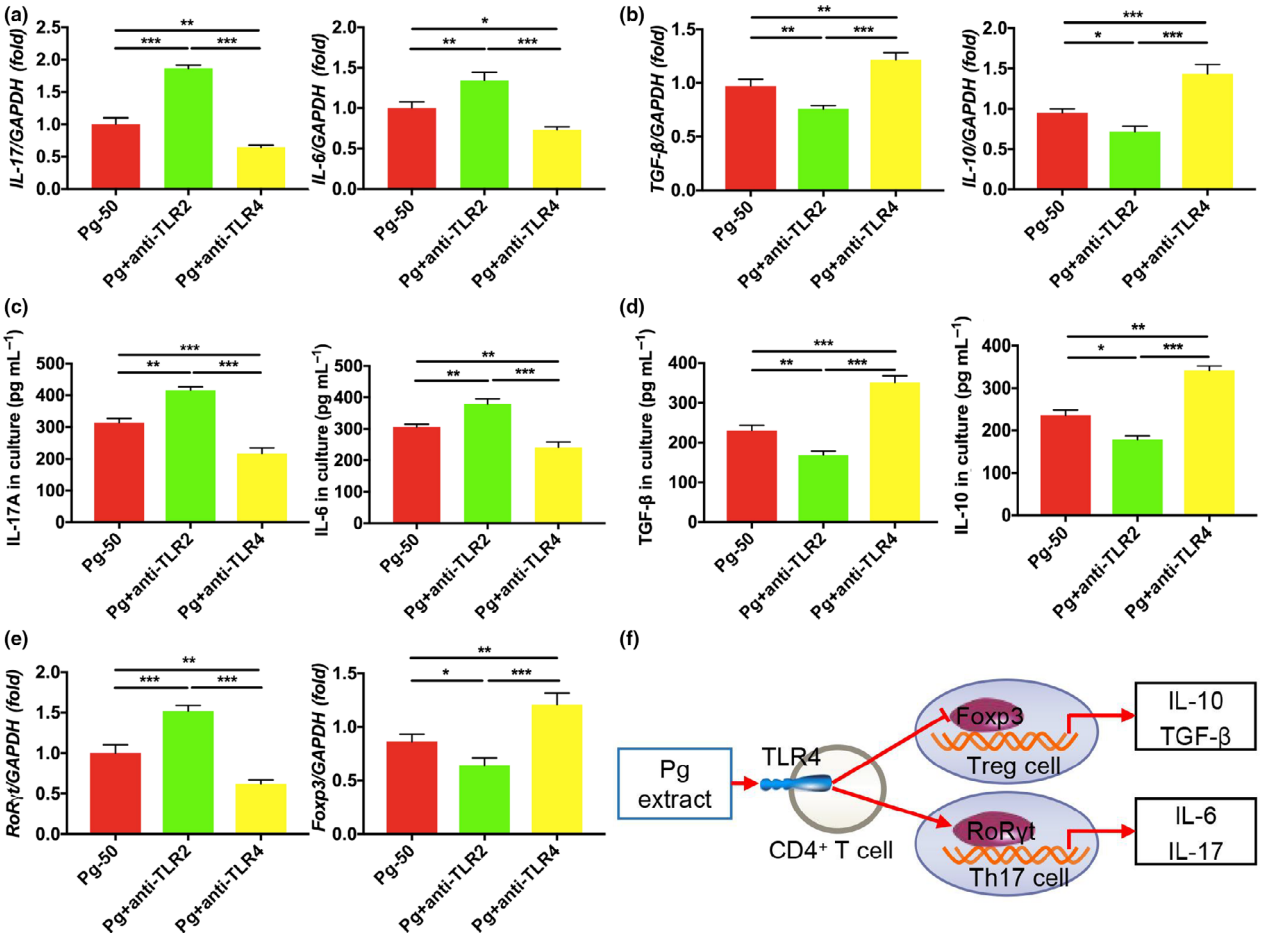


**Figure 2.** Pg ultrasonicate upregulates the Th17 transcription factor and cytokines and downregulates the Treg transcription factor and cytokines via the TLR4 pathway. TLR4 or TLR2 blocking antibodies were used to pretreat $CD4^+$ T cells for 2 h; then, the bacterial extract was added. Target gene expression was measured by the fold change relative to the internal reference gene GAPDH. The culture supernatant of $CD4^+$ T cells stimulated with the bacterial ultrasonicate for 5 days was used for ELISA detection. **(a)** Gene expression and **(c)** protein secretion of the Th17-related cytokines IL-17 and IL-6 were detected via RT-qPCR and ELISA, respectively. **(b)** Gene expression and **(d)** protein secretion of the Treg-secreted cytokines TGF-β and IL-10 were detected via RT-qPCR and ELISA, respectively. **(e)** Gene expression of RoRγt (the essential transcription factor for Th17 differentiation) and Foxp3 (the transcription factor necessary for Treg differentiation) in each group after coculture for 24 h was investigated via RT-qPCR. **(f)** Schematic diagram of Pg ultrasonicate-induced increase in the Th17/Treg ratio mediated by TLR4. The data represent three repeated independent experiments and are shown as the mean ± SD (Bonferroni's multiple comparisons test; $*P < 0.05$; $**P < 0.01$; $***P < 0.001$; NS, no significant difference).

Pg + LGG + anti-TLR2-stimulated system further confirmed the above conclusion (detailed in Supplementary figure 5).

Thus far, we can conclude that the Pg extract increases $CD4^+$ T-cell differentiation into Th17 cells and restrains Treg development via the TLR4 pathway. These results can be overturned after LGG activated the TLR2 pathway, resulting in a decrease in RoRγt and proinflammatory IL-17 and IL-6 production, and an increase in Foxp3 expression and anti-inflammatory TGF-β and IL-10 production (a schematic diagram is shown in Figure 3f).

## Transfer of Pg extract-stimulated $CD4^+$ T cells aggravated and transfer of Pg + LGG-stimulated $CD4^+$ T cells alleviated DSS-induced colitis

We chose the DSS-induced colitis model for *in vivo* experiments to explore how pathogenic and probiotic bacteria's effects on the Th17/Treg balance regulate inflammatory diseases.[23] $CD4^+$ T cells stimulated with different bacterial ultrasonicates were injected intravenously ($1 \times 10^6$ cells per mouse) two days before giving mice 3%

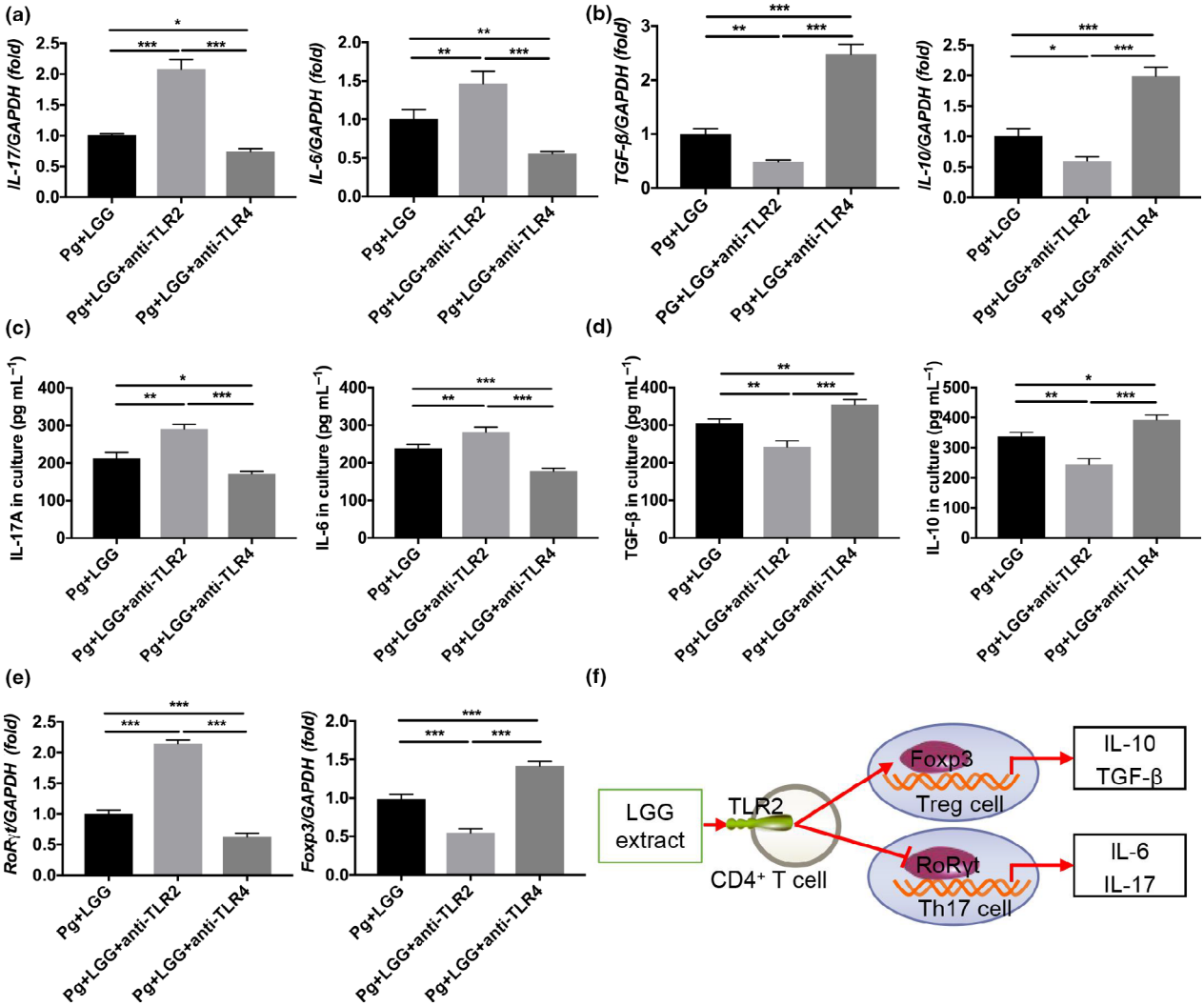


**Figure 3.** Pg extract upregulates RoRγt, IL-17 and IL-6 expression but downregulates Foxp3, TGF-β and IL-10 expression through TLR4, which was reversed by LGG ultrasonicate via TLR2. A TLR2 or TLR4 antagonist was added to the mixed Pg + LGG extract-stimulated $CD4^+$ T cells as mentioned above to detect the gene expression and protein secretion of Th17/Treg-related transcription factors and cytokines. The gene expression of the Th17-related cytokines IL-17 and IL-6 **(a)** and Treg-secreted cytokines TGF-β and IL-10 **(b)** was detected by RT-qPCR after coculture with the microbial ultrasonicate for 24 h. **(c, d)** Protein secretion of IL-17, IL-6, TGF-β and IL-10 in the cell culture supernatant was detected by ELISA after coculture for 5 days. **(e)** Gene expression of RoRγt (essential transcription factor for Th17 differentiation) and Foxp3 (necessary transcription factor for Treg differentiation) in each group was investigated via RT-qPCR. **(f)** Schematic diagram of LGG ultrasonicate-induced reduction in the Th17/Treg balance mediated by TLR2 after the balance was disrupted by Pg. The expression of target genes was measured as the fold change relative to the internal reference gene GAPDH. The data represent three repeated independent experiments and are shown as the mean ± SD (Bonferroni's multiple comparisons test; $*P < 0.05$; $**P < 0.01$; $***P < 0.001$).

DSS, and animals were sacrificed on the eighth day (the experimental approach is shown in Figure 4a). During DSS administration, the disease activity index (DAI) scores based on body weight, diarrhoea and bleeding were evaluated daily.

The colons of mice in the DSS + Pg-T group were significantly shorter than those of mice in the DSS + phosphate-buffered saline (PBS) group (Figure 4b and c, $P < 0.01$). Nevertheless, the colons of mice in the DSS + Pg-LGG-T group were markedly longer than the DSS + Pg-T group ($P < 0.001$) and even longer than the DSS + PBS group ($P < 0.05$). There was no significant difference in colon length between the DSS + LGG-T group and the DSS + PBS group ($P > 0.05$).

From the sixth day, mice in the DSS + Pg-LGG-T group showed more significant weight loss than

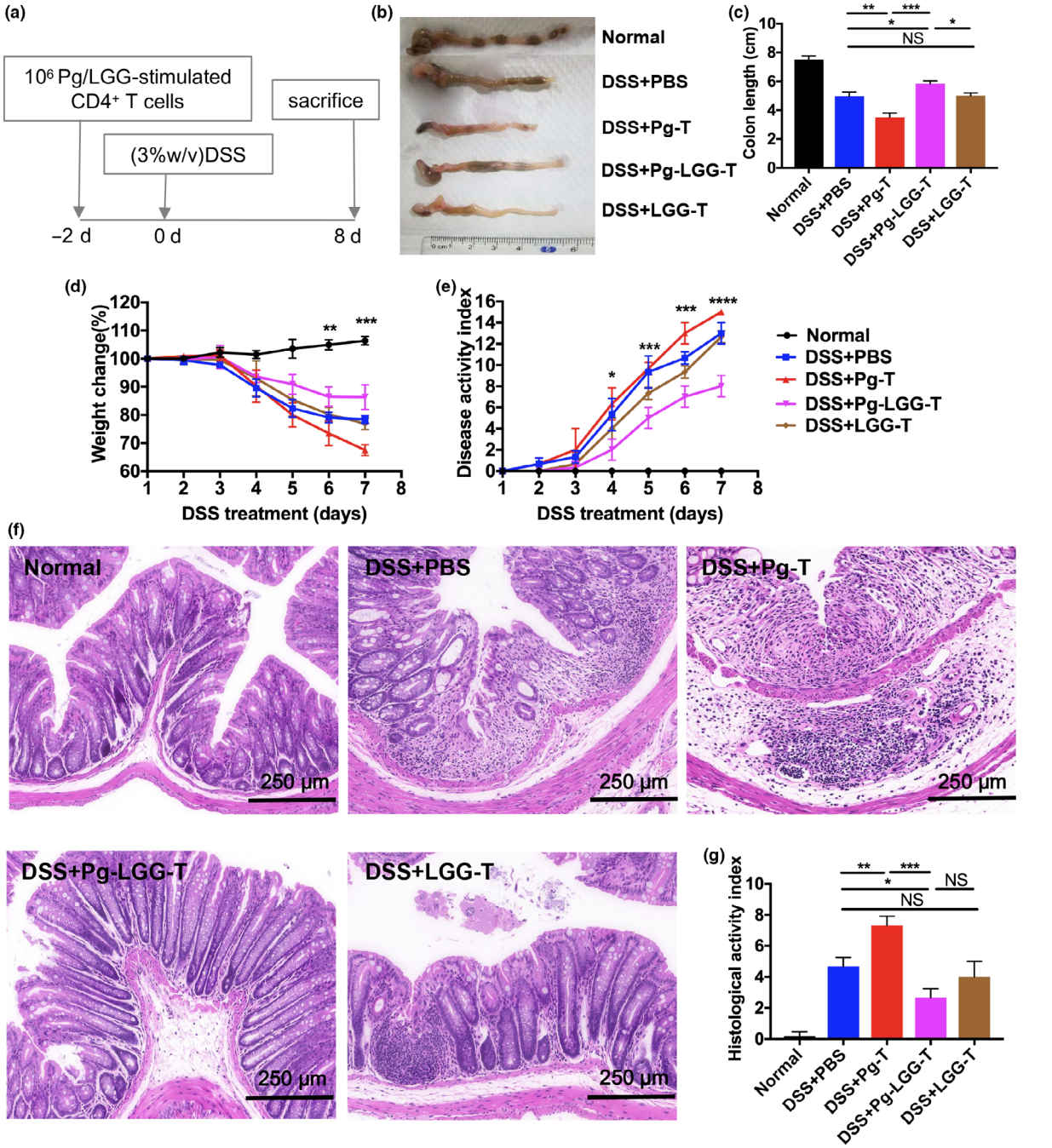


**Figure 4.** Pg extract-stimulated CD4$^+$ T cells aggravated and balanced Pg + LGG-stimulated CD4$^+$ T cells alleviated DSS-induced colitis. Acute colitis was induced in C57BL/6 mice through administration of 3% DSS (w/v) in the drinking water for 7 days; the mice were executed on the eighth day. CD4$^+$ T cells stimulated with different bacterial ultrasonicates were injected intravenously into the mice ($1 \times 10^6$ cells per mouse, $n = 5$) two days before DSS was administered, and the mice were grouped accordingly into the DSS + PBS group, DSS + Pg-T group, DSS + Pg-LGG-T group or DSS + LGG-T group. Mice in the normal group were given normal drinking and no injection. **(a)** Technical schematic for injection of different microbial extract-stimulated CD4$^+$ T cells into DSS-induced colitis mice. **(b)** General view of representative colons and **(c)** statistical analysis of colon length in each group at day 8. **(d)** Weight changes and **(e)** DAI scores of mice were recorded daily and statistically analysed during the DSS administration period. **(f)** H&E staining of representative colons and **(g)** corresponding HAI scores evaluated in each group. Magnification × 100; scale bar = 250 μm. The data are shown as the mean ± SD (Bonferroni's multiple comparisons test; *$P < 0.05$; **$P < 0.01$; ***$P < 0.001$; ****$P < 0.0001$; NS, no significant difference).

mice in the DSS + Pg-T group ($P < 0.01$). The weight of mice in the DSS + Pg-T group was distinctly lower than that of mice in the DSS + PBS group (Figure 4d, $P < 0.01$) on the seventh day. Simultaneously, DAI scores in the DSS + Pg-T group were significantly higher than those in the DSS + PBS group (Figure 4e, $P < 0.05$). Over time, the DAI scores in the DSS + Pg-LGG-T group decreased more significantly than those in the DSS + Pg-T group (Figure 4e, fifth day, $P < 0.01$; sixth day, $P < 0.001$; and seventh day, $P < 0.0001$). Nevertheless, there were no significant differences in weight loss or DAI between the DSS + LGG-T group and the DSS + PBS group ($P > 0.05$).

The histological activity index (HAI) was evaluated according to the loss of goblet cells and crypts and inflammatory cells' infiltration. More than two-thirds of the crypt glands and goblet cells lost in the DSS + Pg-T group, and inflammatory cells were infiltrated into the submucosa, with severe connective tissue oedema (Figure 4f). In contrast, inflammatory symptoms in the DSS + Pg-LGG-T group were significantly reduced. Mucosal folds returned to near-normal, few goblet cells were lost, the lamina propria was dense, and the inflammatory cell infiltration was confined to the glands' periphery. Accordingly, the HAI scores in the DSS + Pg-T group were markedly higher than those in the DSS + PBS group (Figure 4g, $P < 0.01$). The HAI scores in the DSS + Pg-LGG-T group were markedly lower than those in the DSS + Pg-T group ($P < 0.001$) and even lower than those in the DSS + PBS group ($P < 0.05$). The HAI scores in the DSS + LGG-T and DSS + PBS groups were approximately the same ($P > 0.05$). Therefore, we found that Pg-stimulated $CD4^+$ T cells aggravated the inflammatory response, whereas the transfer of the balanced Pg + LGG-stimulated $CD4^+$ T cells alleviated colitis symptoms.

## Transfer of Pg extract-treated $CD4^+$ T cells increased the Th17/Treg ratio in the colon in situ, while the transfer of Pg + LGG extract-treated $CD4^+$ T cells decreased the Th17/Treg ratio

To detect how the transfer of bacterial extract-treated $CD4^+$ T cells to the colon affects the $CD3^+$ IL-$17^+$ Th17 cells and $CD3^+$ $Foxp3^+$ Treg cells in colitis *in situ*, we used immunofluorescence (IF) to visualise and quantitatively analyse the cells. We found that the average percentages of $CD3^+$ IL-$17^+$ Th17 cells and $CD3^+$ $Foxp3^+$ Treg cells per high-power field (HPF) and their ratio in the colon in the DSS + PBS group were notably higher than those in the normal group (Figure 5e, f and g, $P < 0.01$, $P < 0.05$ and $P < 0.05$, respectively), which is indicative of successful construction of a DSS-induced colitis model.[24]

The percentage of *in situ* $CD3^+$ IL-$17^+$ Th17 cells in the DSS + Pg-T group was markedly higher than that of those in the DSS + PBS group (Figure 5a and b, $P < 0.001$), whereas the percentage of $CD3^+$ $Foxp3^+$ Tregs in the DSS + Pg-T group was significantly lower than that of those in the DSS + PBS group (Figure 5c and d, $P < 0.05$), resulting in an extreme increase in the Th17/Treg ratio (Figure 5g, $P < 0.001$). In contrast, the percentage of $CD3^+$ IL-$17^+$ Th17 cells in the DSS + Pg-LGG-T group was markedly lower than that of those in the DSS + PBS group ($P < 0.05$), and the percentage of $CD3^+$ $Foxp3^+$ Treg cells was significantly elevated ($P < 0.01$), bringing about a noticeable reduction in the Th17/Treg ratio ($P < 0.05$). Moreover, the reversal effects in the DSS + Pg-LGG-T group were even more significant than those in the DSS + Pg-T group (Figure 5e–g, $P < 0.001$, $P < 0.001$ and $P < 0.001$, respectively). No significant difference was observed between the DSS + PBS group and the DSS + LGG-T group in terms of $CD3^+$ IL-$17^+$ Th17 cells and $CD3^+$ $Foxp3^+$ Treg cells ($P > 0.05$).

## Reinfusion of TLR2-blocked Pg + LGG extract-stimulated $CD4^+$ T cells upregulated the Th17/Treg ratio in the colon, while reinfusion of TLR4-blocked Pg + LGG extract-stimulated $CD4^+$ T cells did not affect the Th17/Treg ratio

To validate the conclusion that Pg and LGG ultrasonicate modulated the Th17/Treg ratio via TLR4 and TLR2, respectively, we added TLR2/TLR4 antagonists of Pg + LGG-stimulated $CD4^+$ T cells before transfer into the DSS-induced colitis model with the following groups: (1) DSS + PBS group; (2) DSS + Pg-LGG-T group; (3) DSS + Pg-LGG-$T^{anti\text{-}TLR2}$ group; and (4) DSS + Pg-LGG-$T^{anti\text{-}TLR4}$ group. The DSS + Pg-LGG-$T^{anti\text{-}TLR2}$ group showed the most severe signs of inflammation (Figure 6a and d). A loss of approximately 2/3 of the crypt glands was observed in the mucosa, the goblet cells were widely lost, and inflammatory cell infiltration reached the submucosa, with severe connective tissue oedema. The degree of

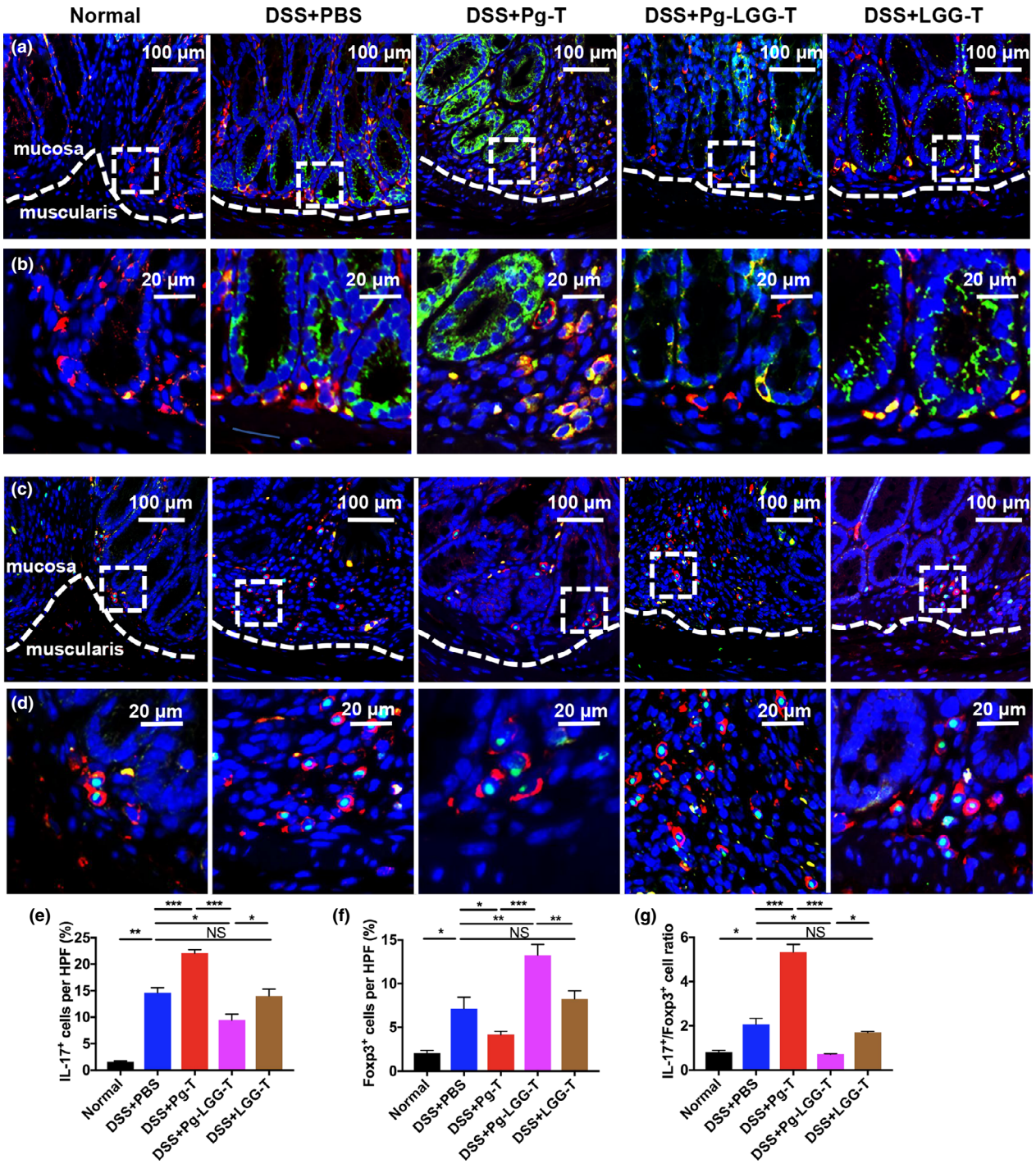


**Figure 5.** Reinfusion of Pg extract-stimulated $CD4^+$ T cells upregulated the Th17/Treg ratio in the colon *in situ*; reinfusion of Pg + LGG extract-stimulated $CD4^+$ T cells downregulated the Th17/Treg ratio in the colon *in situ*. DSS-induced colitis mice were injected via the caudal vein with different microbial extract-stimulated $CD4^+$ T cells. **(a)** The $CD3^+$ $IL\text{-}17^+$ Th17 cells and **(c)** the $CD3^+$ $Foxp3^+$ Treg cells in the colons of mice in each group were visualised *in situ* via IF staining. Red for CD3; green for IL-17 or Foxp3; and blue for DAPI. Magnification × 200; scale bar = 100 μm. Local high-power field (HPF) showing **(b)** $CD3^+$ $IL\text{-}17^+$ Th17 cells and **(d)** $CD3^+$ $Foxp3^+$ Treg cells. Magnification × 400; scale bar = 20 μm. The **(e)** $CD3^+$ $IL\text{-}17^+$ Th17 cell and **(f)** $CD3^+$ $Foxp3^+$ Treg cell positivity rate and **(g)** the corresponding Th17/Treg ratio in five random HPFs were statistically analysed using ImageJ software. The data are shown as the mean ± SD (Bonferroni's multiple comparisons test; $*P < 0.05$; $**P < 0.01$; $***P < 0.001$; NS, no significant difference).

inflammation in the DSS + Pg-LGG-T$^{anti\text{-}TLR4}$ group was similar to that in the DSS + PBS group (Figure 6a and d, $P > 0.05$), showing that the crypt glands arranged irregularly and the inflammatory infiltration was limited around the glands.

Immunofluorescence staining results showed that the percentage of $CD3^+$ $IL\text{-}17^+$ Th17 cells in the colon in the DSS + Pg-LGG-T$^{anti\text{-}TLR2}$ group was significantly higher than that of those in the DSS + Pg-LGG-T group (Figure 6b and e, $P < 0.001$), while the percentage of $CD3^+$ $Foxp3^+$ Treg cells in the colon in the DSS + Pg-LGG-T$^{anti\text{-}TLR2}$ group was lower than that of those in the DSS + Pg-LGG-T group (Figure 6c and f, $P < 0.001$), and the ratio of Th17/Treg cells was significantly increased (Figure 6g, $P < 0.001$). No significant differences were observed in $CD3^+$ $IL\text{-}17^+$ Th17 cells and $CD3^+$ $Foxp3^+$ Treg cells between the DSS + PBS group and the DSS + Pg-LGG-T$^{anti\text{-}TLR4}$ group ($P > 0.05$).

When adding the TLR2 antagonist to the Pg + LGG extract-stimulated $CD4^+$ T-cell system before transfer (the DSS + Pg-LGG-T$^{anti\text{-}TLR2}$ group), the LGG-mediated TLR2 signalling pathway was blocked, and only the Pg-mediated TLR4 signalling pathway played a role, which caused upregulation of Th17 cells and downregulation of Treg cells. For the DSS + Pg-LGG-T$^{anti\text{-}TLR4}$ group, blocking the Pg-mediated TLR4 pathway in the Pg + LGG-stimulated $CD4^+$ T-cell system had effects equivalent to those observed in the DSS + LGG-T group, which showed no significant differences in the DSS + PBS group. These *in vivo* experiments confirmed that Pg mediated the Th17/Treg balance via the TLR4 pathway, while LGG mediated the effects via the TLR2 signalling pathway.

## Microbial extract-treated $CD4^+$ T cells regulated the Th17/Treg ratio in colitis via the JAK-STAT signalling pathway

We also investigated the Th17 and Treg proportions in related immune tissues, including colonic lamina propria lymphocytes (LPLs), mesenteric lymph node (MLN) cells and splenic lymphocytes (SPLs). The percentage of Th17 cells among the LPLs in the DSS + Pg-T group was markedly higher than that of those in the DSS + PBS group (Figure 7a and c, $P < 0.05$), while the Treg proportion among LPLs in the DSS + Pg-T group was significantly lower than that in the DSS + PBS group (Figure 7b and d, $P < 0.05$), resulting in a higher ratio of Th17 to Treg cells (Figure 7e, $P < 0.01$). The changes in the DSS + Pg-LGG-T group in the percentage of Th17 and Treg cells and their ratio were reversed compared with the DSS + Pg-T group ($P < 0.001$, $P < 0.001$ and $P < 0.001$). Also, we detected the Th17 and Treg cell proportions among MLN cells and SPLs (detailed in Supplementary figures 6 and 7) and obtained results similar to those obtained for LPLs.

To identify the differentially expressed cytokines and critical signalling pathways regulating the Th17/Treg balance during colitis after transferring the bacterial extract-treated $CD4^+$ T cells, we collected colon samples from mice in the experimental groups for Quantibody cytokine array analysis (QAM-TH17-1-1). The results showed that the differentially expressed cytokines in the Th17 differentiation signalling pathway were IL-17A, IL-17F and IL-6. The IL-17A, IL-17F and IL-6 concentrations in the colons from mice in the DSS + Pg-T group were significantly higher than those in colons from mice in the DSS + PBS group (Figure 7f, $P < 0.05$, $P < 0.01$ and $P < 0.001$, respectively), whereas those in the DSS + Pg-LGG-T group were significantly lower than those in the DSS + PBS group ($P < 0.01$, $P < 0.001$ and $P < 0.001$, respectively), which is consistent with the previous experimental results. Gene Ontology (GO) and Kyoto Encyclopedia of Genes and Genomes (KEGG) enrichment analyses were carried out after the original data were normalised and compared with genome information databases. We found that cytokine–cytokine receptor interactions play the most crucial role in this process (Figure 7g). More specifically, the process of transmitting cell membrane receptor signals to the nucleus mediated by the JAK-STAT signalling pathway regulated the Th17/Treg balance.

## Microbial extract-stimulated $CD4^+$ T cells regulated the Th17/Treg ratio based on the local cytokine milieu they encountered but not the migration of the cells

The mechanism by which the microbial extract-stimulated $CD4^+$ T cells specifically controlled the Th17/Treg balance in colitis after the transfer was unclear. To explore this problem, we injected Pg-stimulated $CD4^+$ T cells into the tail vein of nude

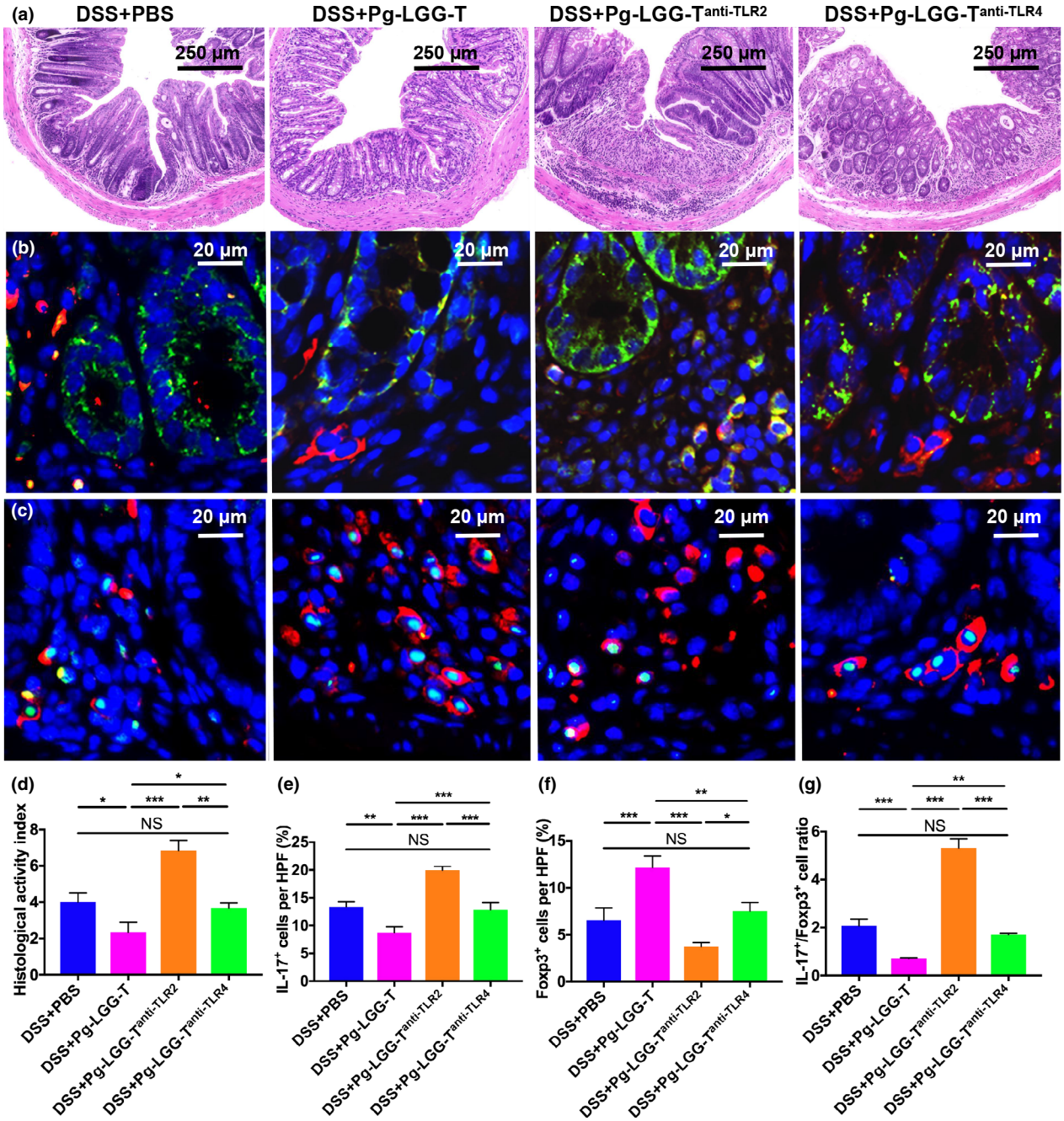


**Figure 6.** Reinfusion of TLR2-blocked Pg + LGG extract-stimulated $CD4^+$ T cells upregulated the Th17/Treg ratio in the colon *in situ*; reinfusion of TLR4-blocked Pg + LGG extract-stimulated $CD4^+$ T cells did not affect the Th17/Treg ratio. Pg + LGG extract-stimulated $CD4^+$ T cells or Pg + LGG-stimulated $CD4^+$ T cells treated with TLR2/TLR4 antagonists were injected into DSS-induced colitis mice via the caudal vein. The mice were grouped accordingly into the DSS + PBS group, DSS + Pg-LGG-T group, DSS + Pg-LGG-$T^{anti\text{-}TLR2}$ group or DSS + Pg-LGG-$T^{anti\text{-}TLR4}$ group. **(a)** H&E staining of representative colons and **(d)** corresponding HAI scores evaluated in each group. Magnification × 100; scale bar = 250 μm. Local high-power field (HPF) showing **(b)** $CD3^+$ $IL\text{-}17^+$ Th17 cells and **(c)** $CD3^+$ $Foxp3^+$ Treg cells with IF staining. Red for CD3; green for IL-17 or Foxp3; and blue for DAPI. Magnification × 400; scale bar = 20 μm. The positive rate of **(e)** $CD3^+$ $IL\text{-}17^+$ Th17 cells and **(f)** $CD3^+$ $Foxp3^+$ Treg cells and **(g)** the corresponding Th17/Treg ratio were statistically analysed in five random HPFs using ImageJ software. The data are shown as the mean ± SD (Bonferroni's multiple comparisons test; $*P < 0.05$; $**P < 0.01$; $***P < 0.001$; NS, no significant difference).

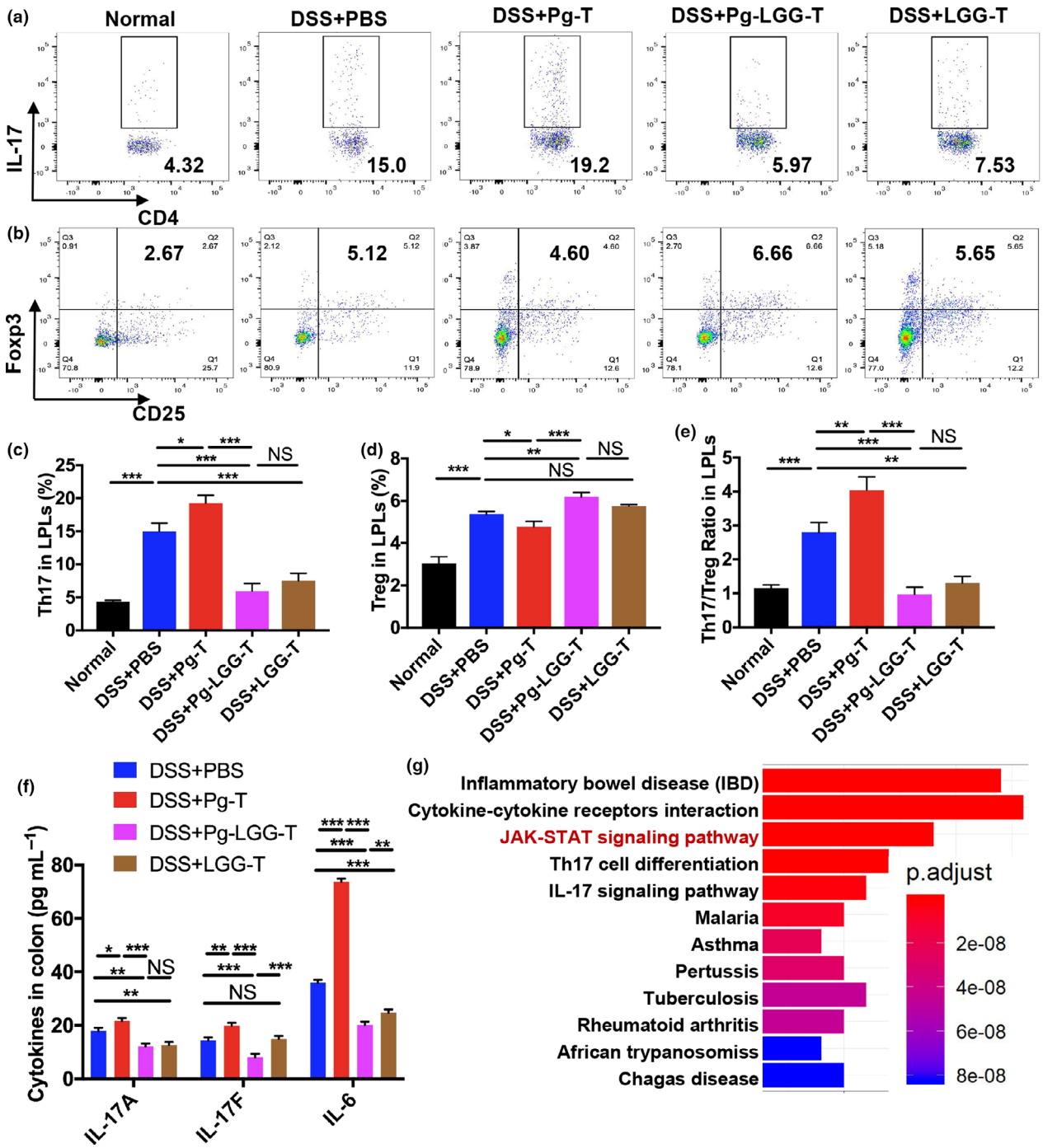


**Figure 7.** Microbial extract-treated CD4$^+$ T cells regulated the Th17/Treg ratio in colitis via the JAK-STAT signalling pathway. DSS-induced colitis mice were injected via the caudal vein with different microbial extract-stimulated CD4$^+$ T cells or PBS (grouped as DSS + PBS, DSS + Pg-T, DSS + Pg-LGG-T and DSS + LGG-T). **(a, c)** The proportion of CD4$^+$ IL-17$^+$ Th17 cells and **(b, d)** the percentage of CD4$^+$ CD25$^+$ Foxp3$^+$ Treg cells among LPLs in each group were detected via flow cytometry and statistically analysed. The normal group included mice without DSS or T-cell injection. **(e)** The relative Th17-to-Treg cell ratio in each experimental group was calculated and statistically analysed. **(f)** The differentially expressed cytokines involved in Th17 cell differentiation in the colons after injection of microbial extract-treated CD4$^+$ T cells were identified with a Quantibody cytokine array, and **(g)** KEGG pathway enrichment analysis was performed to identify key pathways regulating the Th17/Treg balance. The data represent three repeated independent experiments and are shown as the mean ± SD (Bonferroni's multiple comparisons test; *$P < 0.05$; **$P < 0.01$; ***$P < 0.001$; NS, no significant difference).

mice with DSS-induced colitis and detected the proportion of $CD4^+$ T cells in the local colon and related lymphoid tissues and the concentration of Th17/Treg-related cytokines in the colon and peripheral serum.

As shown in Figure 8a and b, no significant changes were found in the proportion of $CD4^+$ T cells between the Nude + DSS + Pg-T group and the Nude + DSS + PBS group, including colonic LPLs, MLNs and SPLs (all $P > 0.05$). These results suggest that the differentiation of reinfused $CD4^+$ T cells into Th17 cells or Tregs in colitis mice was not because of the direct local immune regulation caused by migration of the microbial extract-stimulated $CD4^+$ T cells to the colon. However, the IL-17A and IL-6 concentrations in colonic homogenates from the Nude + DSS + Pg-T group were significantly higher than those in homogenates from the Nude + DSS + PBS group (Figure 8c, Nude + DSS + Pg-T group *versus* Nude + DSS + PBS group, IL-17A, $22.6 \pm 2.75$ pg $mL^{-1}$ *versus* $10.7 \pm 1.53$ pg $mL^{-1}$, $P < 0.01$; IL-6, $64.3 \pm 5.66$ pg $mL^{-1}$ *versus* $26.7 \pm 2.7$ pg $mL^{-1}$, $P < 0.01$). At the same time, the IL-10 and TGF-β concentrations in the Nude + DSS + Pg-T group were significantly lower than those in the Nude + DSS + PBS group (Nude + DSS + Pg-T group *versus* Nude + DSS + PBS group, IL-10, $103 \pm 8.74$ pg $mL^{-1}$ *versus* $62.6 \pm 5.12$ pg $mL^{-1}$, $P < 0.01$; TGF-β, $1615 \pm 104$ pg $mL^{-1}$ *versus* $522 \pm 65.3$ pg $mL^{-1}$, $P < 0.01$). The changes in the corresponding cytokines in serum showed a consistent trend, with the production of IL-17A and IL-6 in the Nude + DSS + Pg-T group being significantly higher than that of those in the Nude + DSS + PBS group, while the production of IL-10 and TGF-β in the Nude + DSS + Pg-T group was significantly lower than that of those in the Nude + DSS + PBS group (Figure 8d, IL-17A and IL-6, $P < 0.01$; IL-10 and TGF-β, $P < 0.01$). Considering the above experimental results, we speculate that the local differentiation of Th17 cells or Treg cells in inflammatory lesions is based on the specific cytokine milieu encountered by the transferred microbial extract-stimulated $CD4^+$ T cells. In other words, intricate interactions between proinflammatory or anti-inflammatory cytokines and cytokine receptors in the inflammatory microenvironment are likely to contribute to the regulation of the Th17/Treg balance, in addition to microbial extract prestimulation of $CD4^+$ T cells.

## DISCUSSION

Many microorganisms reside in the oral environment and intestines of healthy organisms but do not induce inflammation, indicating that the body has a plastic regulatory mechanism to control immune homeostasis. IBD, as a nonspecific mucosal inflammatory disease, is essentially a disturbance in the balance between the microbial ecosystem and host immune system mediated by $CD4^+$ T cells, especially the Th17/Treg equilibrium, which plays a prominent role in disease progression.[25] Therefore, the DSS-induced colitis model is well suited to studying inflammation based on the Th17/Treg balance.[26] We verified that regulation of the Th17/Treg balance among $CD4^+$ T cells stimulated by the Pg and LGG extracts is based on the activation of specific TLRs and modulation of cytokines and specific transcription factors *in vitro*. These microbial extract-stimulated $CD4^+$ T cells also regulated DSS-induced colitis by changing the Th17 and Treg cell balance *in vivo*.

We found that the Pg (ATCC 33277) bacterial extract prepared by ultrasonication and high-speed centrifugation induced activated $CD4^+$ T-cell apoptosis as a type of antigenic stimulus (Figure 1), which is consistent with the conclusions of previous studies. For example, the apoptosis rate of human peripheral blood mononuclear cells (PBMCs) is increased by stimulation with LPS and HmuY protein from Pg.[27] Besides, Pg-related substances cause apoptosis of $CD3^+$ T cells and human gingival epithelial cells by increasing the expression of Fas ligand (FasL).[28,29] In the clinic, the proportion of active $CD4^+$ T cells extracted from adult periodontitis lesions is lower than that of those extracted from healthy subjects.[30] Generally, the T-cell apoptosis following stimulation with pathogenic antigen components decreases autoreactive cells' proportion and the excessive immune response.[31]

However, the effect of probiotics on activated $CD4^+$ T-cell proliferation is controversial because of the different bacterial strains and target cells studied. Even the same *Lactobacillus paracasei* (*L. paracasei*) strain exhibits different effects; for example, the subsp. *paracasei* B21060 inhibits the proliferation of active $CD4^+$ T cells, whereas the subsp. *paracasei* F19 does not influence T-cell viability. Our results show that the LGG ultrasonicate significantly promoted activated $CD4^+$ T-cell proliferation but had no significant apoptosis effects. These findings may explain why

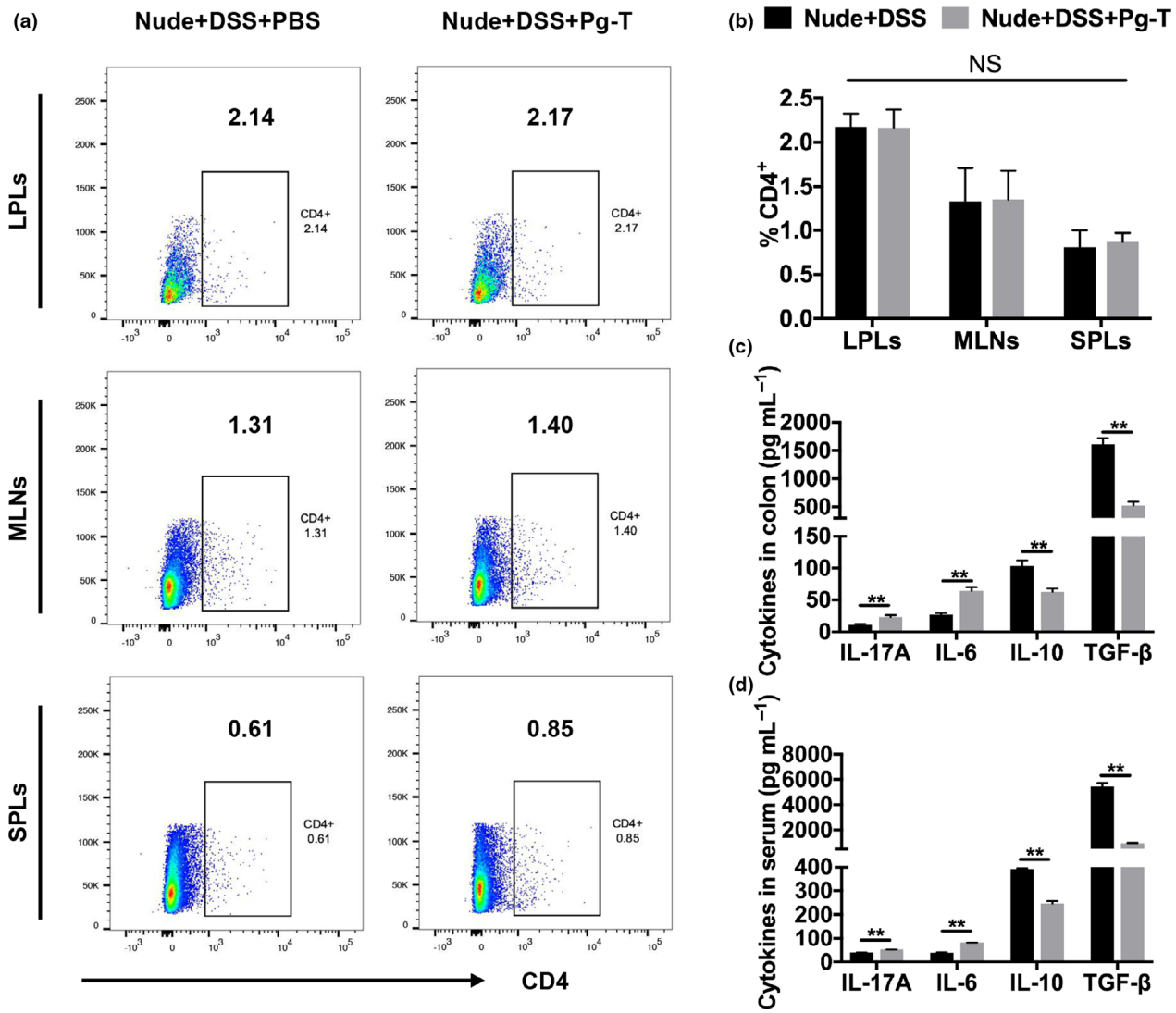


**Figure 8.** Microbial extract-stimulated CD4$^+$ T cells regulated the Th17/Treg ratio based on the local cytokine milieu they encountered but not on migration of the cells. **(a, b)** The proportion of CD4$^+$ cells among colonic lamina propria lymphocytes (LPLs), mesenteric lymph node (MLN) cells and splenic lymphocytes (SPLs) in each group was detected via flow cytometry and statistically analysed after Pg extract-stimulated CD4$^+$ T cells or PBS was injected into DSS-induced colitis nude mice via the caudal vein (grouped as Nude + DSS+Pg-T and Nude + DSS + PBS). The protein secretion of the Th17-related cytokines IL-17 and IL-6 and the Treg-secreted cytokines TGF-β and IL-10 was detected via ELISA in **(c)** the colonic homogenate and **(d)** in serum, respectively. The data represent three repeated independent experiments and are presented as the mean ± SD (Bonferroni's multiple comparisons test; $^{**}P < 0.01$; NS, no significant difference).

different probiotic strains or subspecies show diverse immune regulation effects in inflammatory diseases.[32]

Interestingly, cell viability was improved when active CD4$^+$ T cells were stimulated by the mixed Pg + LGG extract rather than the Pg ultrasonicate alone, indicating that the probiotic LGG prevents Pg from promoting CD4$^+$ T-cell apoptosis. Other studies have shown that the probiotic *Lactobacillus acidophilus* inhibits the apoptosis of LPS-treated human endothelial cells.[33] More importantly, we found that the immunomodulatory effect of the probiotic LGG against pathogenic Pg was also reflected in the maintenance of the Th17 and Treg balance. By activating the TLR4-mediated signalling pathway, Pg ultrasonicate increased the expression of the transcription factor RoRγt, resulting in an increase in Th17 cells and the proinflammatory factors IL-17 and IL-6; at the same time, Pg extract

decreased the expression of the transcription factor Foxp3, resulting in a decrease in Treg cells and the anti-inflammatory factors TGF-β and IL-10. Once the Th17/Treg balance is broken, LGG increases the proportion of Tregs and reduces the proportion of Th17 cells in the $CD4^+$ T-cell system via the TLR2 signalling pathway to maintain the steady state.

Th17 cells are defined as having RoRγt as the critical transcription factor and are capable of secreting the proinflammatory factor IL-17, which plays a critical role in inflammatory and autoimmune disorders.[34] For example, IL-17 directly mediates alveolar bone resorption and aggravation of inflammation in periodontitis animal models induced by Pg.[35] We already knew that the IL-6-mediated JAK-STAT3 axis leads to the upregulation of RoRγt and RoRα, which triggers Th17 cells to secrete many natural cytokines, including IL-17A, IL-17F and IL-22.[36] Our experiments showed that Pg ultrasonicate significantly increased the percentage of Th17 cells and IL-17 and IL-6 expression, which further verified the above conclusion.

Treg cells with negative immune regulation activity are usually divided into two categories: natural Tregs (nTregs) and inducible Tregs (iTregs), with the former accounting for the majority of Treg cells in peripheral, and the latter primarily appearing in culture or at microorganism–host interfaces, such as in the intestinal tract.[37] Tregs and Th17 cells are closely related and interchangeable. Many $Foxp3^+$ Treg cells in the intestine express a large amount of RoRγt and produce IL-17, and more than a quarter of $IL\text{-}17^+$ Th17 cells express Foxp3 at a specific stage in their *in vivo* development. The IL-2-mediated JAK-STAT5 pathway inhibits Th17 differentiation but promotes Treg differentiation *in vitro*.[38,39] These discoveries are in agreement with our conclusion that Pg ultrasonicate simultaneously induces an increase in the Th17 population and a decrease in the Treg population.

A recent study identified a subpopulation of $CD4^+$ T cells defined as Treg17 cells, which can express both Foxp3 and IL-17 under variable inflammatory conditions. These IL-17-producing Treg cells originate from the $CD4^+$ T-cell population induced by TGF-β and IL-6 *in vitro* and express RoRγt and IL-10.[36] Three determinants affected the transition between general Th17 cells and Treg cells: specific transcription factors, cytokines and TLRs.[40] Regarding transcription factors and cytokines, TGF-β plays a particularly important role because its synergistic effect with different cytokines determines the production of Foxp3 or RoRγt.[40] In detail, when TGF-β works together with the IL-2-STAT5 pathway, Foxp3 expression is induced[41]; when TGF-β cooperates with the IL-6-STAT3 pathway, RoRγt expression is induced.[42] Moreover, TGF-β induces intestinal activated $CD4^+$ T cells to differentiate into $IL\text{-}10^+$ $Foxp3^+$ Treg cells *in vitro*.[43] In our experiments, increased RoRγt, IL-17 and IL-6 expression and decreased Foxp3, IL-10 and TGF-β expression appeared concurrently in the Pg-stimulated $CD4^+$ T-cell culture system. After the LGG ultrasonicate neutralised the Pg extract, the Foxp3, IL-10 and TGF-β transcription levels increased, and RoRγt, IL-17 and IL-6 expression decreased, contributing to the maintenance of the Th17/Treg equilibrium.

TLR2 and TLR4 are the most widely studied association with Pg because of its heterogeneous lipid A structure. Generally, the leading bacterial components recognised by TLR2 are lipopeptides and lipoteichoic acid (LTA) of $gram^+$ bacteria, whereas the primary substance detected by TLR4 is the endotoxin LPS from $gram^-$ bacteria.[44] Our experiments demonstrate that Pg ultrasonicate increased the Th17 proportion and decreased the Treg proportion through the TLR4-mediated signalling pathway *in vitro*. If the TLR4 signalling pathway was blocked before Pg + LGG-stimulated $CD4^+$ T cells were reintroduced, its role in regulating the Th17/Treg balance in the colon *in vivo* was consistent with that of $CD4^+$ T cells stimulated by LGG alone, which inversely verified that Pg regulates the Th17/Treg balance through the TLR4-mediated signalling pathway. Other studies have shown that LPS (the effective ligand of TLR4) selectively promotes secretion of the proinflammatory cytokine IL-17 mediated by IL-6, and the severity of inflammation is negatively correlated with the proportion of Treg cells, which is consistent with our results.[45]

However, the bacterial lipoprotein Pam3Cys-SK4 (a specific TLR2 agonist) directly promotes Treg proliferation without APCs and converts conventional Tregs into Treg17 cells.[46,47] Our experiments also demonstrate that LGG ultrasonicate increases Treg differentiation and decreases Th17 differentiation via the TLR2-mediated signalling pathway on the $CD4^+$ T-cell surface *in vitro*. If the TLR2 signalling pathway was blocked before Pg + LGG-stimulated $CD4^+$ T cells were reintroduced, its role in regulating the

Th17/Treg balance in the colon *in vivo* was consistent with that of $CD4^+$ T cells stimulated by Pg alone, which inversely verified that LGG regulates the Th17/Treg balance through the TLR2-mediated signalling pathway. Therefore, TLR4 and TLR2 were confirmed to be involved in regulating the Th17/Treg balance in our experimental results.

When $CD4^+$ T cells isolated from an individual with autoimmune disease are injected into normal mice, experimental autoimmune encephalomyelitis (EAE) and diabetes occur.[48,49] Besides, colitis can be induced by injecting $CD4^+CD45RB^{hi}$ T cells (a subset separated from whole $CD4^+$ T cells) into severe combined immunodeficiency (SCID) mice, which is another common way to establish an experimental colitis model. However, the transfer of whole $CD4^+$ T-cell samples (unseparated) ameliorates colitis.[50] This evidence suggests the importance of maintaining the balance between $CD4^+$ T-cell subsets to prevent immune disorders and associated inflammation. Furthermore, a recent study found that transfer of Treg-ablated $CD4^+$ T cells induced colitis, suggesting that the impaired immunosuppressive function of Treg cells and the overactivation of inflammatory effector cells are critical mechanisms for colitis.[51] In our experiments, an increased Th17 cell percentage and a decreased Treg percentage in the $CD4^+$ T-cell culture were induced by Pg extract via the TLR4-mediated pathway *in vitro*. Reinfusion of these imbalanced $CD4^+$ T cells aggravated colitis and further increased the Th17/Treg ratio *in situ* and LPLs. In contrast, the balance between Th17 cells and Treg cells was restored in $CD4^+$ T cells via the TLR2-mediated pathway after *in vitro* stimulation with Pg + LGG mixed extract. When these cells with a well-balanced Th17/Treg subgroup were injected back into mice with colitis, the inflammatory symptoms were alleviated, based on the increased colon length and the decreased DAI and HAI scores.

Furthermore, we found that the JAK-STAT signalling pathway directly regulates the Th17/Treg balance during this process. The JAK-STAT pathway plays a vital role in the arrangement of cytokine receptors, regulating the differentiation of helper T cells.[52] STAT3 is necessary for the specific transcription factor RORγt to induce Th17 cell differentiation,[53] and STAT5 promotes Treg differentiation by binding to the promoter of the *Foxp3* gene.[54] Therefore, we speculate that the induction of Th17/Treg balance in colitis by transferring microbial extract-stimulated $CD4^+$ T cells is essentially the RORγt/Foxp3 balance regulated by the JAK-STAT3/STAT5 signalling pathway. The trigger of the JAK-STAT signalling pathway can be traced back to the interaction between the extracellular cytokines in the cytokine pool and the cytokine receptors on the cell membrane, rather than to a direct effect of microbial extract-stimulated $CD4^+$ T cells with a regulated Th17/Treg balance. These findings showed that the transfer of microbial extract-stimulated $CD4^+$ T cells did not increase the $CD4^+$ T-cell ratio in the colon and MLNs. However, it caused significant changes in the content of proinflammatory cytokines and anti-inflammatory cytokines in the colon and serum.

Indeed, the Th17/Treg balance plays a leading role in the pathogenesis of many mucosal inflammatory diseases in addition to colitis. Our data suggest that pathogenic Pg and probiotic LGG directly regulate the Th17/Treg balance among the $CD4^+$ T-cell system through different TLRs. It provides a theoretical basis for follow-up studies of the pathogenesis and treatment of oral inflammatory diseases with Pg as the core and for treating inflammation to reduce the proinflammatory Th17 cell population and improve the immunosuppressive function of Treg cells. However, a more detailed understanding of what substances in bacterial extracts at the molecular level regulate the Th17/Treg balance and immune responses in inflammatory diseases via specific TLRs requires in-depth analysis.

# METHODS

## Ethics statement

All animal procedures were carried out under approved guidelines developed by the Animal Ethics Committee of the School of Stomatology, Capital Medical University (Beijing, China). All animal experiments were conducted according to the agency-approved protocols for animal research (Capital Medical University #KQYY-201712-002).

## Culture of Pg and LGG

Pg strain ATCC 33277 and LGG strain CICC 6141 were used in this study. Both strains were preserved and revived by the Laboratory of Tissue Regeneration and Immunology and the Department of Periodontics, School of Stomatology, Capital Medical University. Pg was grown on CDC anaerobic agar medium (AOBOX, Beijing, China) with 5 mg $L^{-1}$ haematin chloride (Solarbio, Beijing, China),

500 g $L^{-1}$ vitamin K (Shyndec Pharmaceutical Co., Ltd, Shanghai, China), 5% defibrillated sheep blood and 0.1% L-cysteine hydrochloride (Dingguo Biotechnology Co., Ltd, Beijing, China), and cultured under anaerobic conditions (80% $N_2$, 10% $CO_2$ and 10% $H_2$) at 37°C. The probiotic LGG was cultured on MRS agar medium (AOBOX) at 37°C under anaerobic conditions. The purity of the bacteria was verified by Gram staining and phase-contrast microscopy.

## Preparation of the bacterial ultrasonicate

Logarithmic growth phase (Pg) and LGG bacteria were collected with cell scrapers into separate 50-mL centrifuge tubes of known weights containing PBS (pH 7.4) and centrifuged at 27 000 *g* for 5 min at 4°C. After removing the supernatant, the difference in the centrifuge tubes' weight before and after was calculated to obtain the bacteria's total weight. The bacterial cell pellet was washed twice with PBS and resuspended in a specific volume of sterile deionised water to calculate the bacterial extract concentration according to the mass-to-volume ratio. Using a JYD-150 ultrasonic cell disruptor (Zhixin Instrument Co., Ltd, Shanghai, China) at maximum power, the bacteria were thoroughly lysed. Then, the insoluble debris was removed by centrifugation at 10 000 *g* for 15 min at 4°C, and the supernatant was sterilised via filtration through 0.22-μm-pore-size filters (Millipore, Massachusetts, USA) and stored at −80°C.[55]

## Isolation and culture of $CD4^+$ T cells

Unless otherwise stated, cells were cultured in RPMI 1640 medium (Gibco, New York, USA) containing 10% foetal bovine serum (FBS; HyClone, Los Angeles, USA), 1% 1 M HEPES, 2 mM glutamine (Sigma-Aldrich, Milwaukee, USA), 100 U $mL^{-1}$ penicillin (Sigma-Aldrich), 0.1 mg $mL^{-1}$ streptomycin (Sigma-Aldrich), 1% 100 × sodium pyruvate and 2 μM 2-mercaptoethanol (Invitrogen, Carlsbad, USA) in a humidified atmosphere (37°C and 5% $CO_2$). Activated $CD4^+$ T cells were purified magnetically from splenocytes isolated from wild-type C57BL/6 mice aged 6–8 weeks (purity > 90%) using a $CD4^+$ T-cell Isolation Kit (Miltenyi Biotec, Bergisch Gladbach, Germany) and cultured at $1 \times 10^6$ per well in the presence of plate-bound anti-CD3 antibody (2 μg $mL^{-1}$, Biolegend, California, USA) and soluble anti-CD28 antibody (2 μg $mL^{-1}$, Biolegend) for activation.[56] Inactive $CD4^+$ T cells were cultured in the absence of anti-CD3 and anti-CD28 antibodies. Different concentrations of Pg or LGG bacterial extracts were added to the culture medium to stimulate cells for subsequent detection via flow cytometry, RT-qPCR or enzyme-linked immunosorbent assay (ELISA).

## Detection of proliferation and apoptosis

Pg and/or LGG ultrasonicate was added to activated or nonactivated $CD4^+$ T-cell culture systems at a final concentration of 25 μg $mL^{-1}$, 50 μg $mL^{-1}$ or 100 μg $mL^{-1}$ alone or at a ratio of 1:1.

For proliferation tests, parental $CD4^+$ T cells were labelled with carboxyfluorescein succinimidyl ester (CFSE) using a CellTrace™ CFSE Cell Proliferation Kit (Invitrogen) according to the manufacturer's instructions; then, the extract was added. Forty-eight hours later, the $CD4^+$ T cells were collected and analysed via flow cytometry. The obtained data were analysed using ModFit LT™ software, and cell proliferation was statistically analysed.

For apoptosis tests, an Annexin V/PI Apoptosis Kit (BD Pharmingen, New York, USA) and flow cytometry were used according to the manufacturer's protocols to detect the apoptosis rate of $CD4^+$ T cells stimulated with bacterial ultrasonicate. The apoptosis rates were analysed using FlowJo software.

## TLR blocking assay

We applied a TLR blocking assay as previously described to explore the role of TLR4/TLR2 in the regulation of the Th17/Treg balance among $CD4^+$ T cells stimulated with bacterial extracts.[57] Two hours before the activated $CD4^+$ T cells were stimulated with the bacterial extracts, a TLR2 or TLR4 antagonist (Biolegend) at a final concentration of 10 μg $mL^{-1}$ was added to the culture system to block TLR4 or TLR2.

## Detection of Th17/Treg cells via flow cytometry

Treg cells were characterised by the expression of the specific transcription factor Foxp3 and surface activation marker CD25. After being labelled with FITC anti-mouse CD4 and APC anti-mouse CD25 antibodies (Biolegend), the cells were stained with fixation/permeabilisation buffer (eBioscience, California, USA) according to the manufacturer's instructions and then labelled with a PE anti-mouse Foxp3 antibody (Biolegend). For Th17 cell staining, cells were stimulated at 37°C for 5 h with a Cell Activation Cocktail containing Brefeldin A (Biolegend) and then labelled with a FITC anti-mouse CD4 antibody. After being permeabilised with intracellular staining fixation/permeabilisation buffer (Biolegend) according to the manufacturer's instructions, the cells were stained with a PE anti-mouse IL-17 antibody (Biolegend).[58] The stained cells were detected using an LSRFortessa cell analyser (BD, New York, USA). The data were analysed with FlowJo software, and the Th17 and Treg cell percentages among the total $CD4^+$ T cells and the Th17/Treg ratio were statistically analysed.

## Gene expression and cytokine secretion

The gene expression levels of Th17- and Treg-related cytokines (IL-17, IL-6, TGF-β and IL-10) and the corresponding key transcription factors (RoRγt and Foxp3) were detected via reverse transcription–quantitative PCR (RT-qPCR; TaKaRa, Beijing, China). The housekeeping gene GAPDH was used as an internal reference control gene. The culture supernatant of $CD4^+$ T cells stimulated with the bacterial ultrasonicate for 5 days was preserved to detect cytokines' secretion (IL-17, IL-6, TGF-β and IL-10) via ELISA. The operation was carried out according to the kit instructions (Biolegend).

## Animals

Female specific-pathogen-free (SPF) C57BL/6 mice (8 weeks old) were purchased from Beijing HFK Bioscience Co., Ltd and raised in a 12-h day/night environment at 25°C with access to a standard diet and drinking water. Before animal experiments were conducted, the mice were allowed to adapt to the environment for a week.

## Establishment of the DSS-induced acute colitis model

Acute colitis was induced in C57BL/6 mice by ingestion of 3% (w/v) DSS (MP Biochemicals, Santa Ana, USA) in drinking water.[59] Two days before DSS administration, $1 \times 10^6$ $CD4^+$ T cells treated with equal amounts of Pg, LGG or Pg + LGG bacterial ultrasonicate in 200 μL of PBS were injected into each mouse via the tail vein (five mice in each group). Accordingly, the mice were divided into the following groups: the DSS group (no cell injection), the DSS + PBS group (injection of PBS), the DSS + Pg-T group (injection of $CD4^+$ T cells stimulated with Pg extract), the DSS + Pg-LGG-T group (injection of $CD4^+$ T cells stimulated with mixed Pg + LGG extract), the DSS + LGG-T group (injection of $CD4^+$ T cells stimulated with LGG extract) and the normal group (healthy mice without DSS or T-cell injection). Weight changes and the DAI of mice in each group were measured daily. Mice were sacrificed on the 8th day of continuous DSS administration, and the length of the colon was measured. Animal specimens were processed as previously described.[60]

## Measurement of weight and DAI

The severity of mouse colitis in different groups was judged by daily body weight and DAI assessment. The DAI calculation method was as previously described.[61] Changes in body weight were scored according to the following criteria: 0 points (none), 1 point (1–5%), 2 points (6–10%), 3 points (11–15%), 4 points (16–20%), 5 points (21–25%) and 6 points (26-30%). The faecal scoring criteria were as follows: 0 points (normal), 1 point (mildly soft), 2 points (loose stool), 3 points (diarrhoea) and 4 points (watery diarrhoea). The bleeding was scored as follows: 0 points (no bleeding), 2 points (minor bleeding) and 4 points (severe bleeding). DAI scores ranged from 0 (unaffected) to 14 (severe colitis).

## Evaluation of the histological activity index (HAI)

Colons were fixed in 4% paraformaldehyde solution, embedded in paraffin, cut into 4 μm sections and stained with H&E. HAI was assessed according to the loss of goblet cells and crypts and the extent of inflammatory cell infiltration.[16] Crypt gland destruction was scored as follows: 0 points (normal), 1 point (a small amount of crypt loss), 2 points (a large amount of crypt loss) and 3 points (extensive crypt loss). Goblet cell loss was scored as 0 points (normal), 1 point (small), 2 points (large) and 3 points (most). Inflammatory cell infiltration was scored as 0 points (normal), 1 point (infiltration around crypt glands), 2 points (infiltration of the mucosal muscle layer), 3 points (extensive infiltration of the mucosal muscle layer with oedema) and 4 points (infiltration of the submucosal layer). The histological scores of each group were summed to obtain a total score of 0–10.

## Immunofluorescence of Th17 and Treg cells in situ

The colons obtained from mice in different groups were cut into tissue sections with a thickness of 8 μm using a frozen microtome (Leica, Wetzlar, Germany). The sections were incubated with a buffer containing 5% normal blocking serum (ZSGB-bio, Beijing, China) for 1 h. Then, the sections were incubated overnight at 4°C with a primary antibody against CD3 (1:50, Santa Cruz, Dallas, USA) mixed with an antibody against IL-17 (1:200, Abcam, Cambridge, England) or with an antibody against CD3 (1:50) mixed with an antibody against Foxp3 (1:100, Cell Signaling Technology, Danvers, USA). After being washed, the sections were incubated with corresponding biotinylated Alexa Fluor 555-labelled (red) and 488-labelled (green) secondary antibodies (Beyotime, Shanghai, China). The sections were then counterstained with DAPI (Beyotime), sealed with antifade mounting medium (Beyotime) and observed via fluorescence microscopy.[62] Five fields of view were randomly selected to calculate the $CD3^+$ $IL\text{-}17^+$ Th17 cell and $CD3^+$ $Foxp3^+$ Treg cell proportions using ImageJ software.

## Acquisition of lamina propria lymphocytes (LPLs)

Briefly,[63] mouse colons were longitudinally dissected, shaken with PBS to remove faeces, cut into 5-mm fragments and stirred with PBS containing 5 mM EDTA and 1 mM DTT for 30 min at 37°C. After being filtered through 70-μm filters, the tissues were mixed with PBS containing 5 mM EDTA and 1 M HEPES and shaken vigorously for 1 min. This step was repeated three times. Then, all tissue pieces were collected and stirred with PBS containing 2500 U $mL^{-1}$ collagenase D (Roche, Basel, Switzerland), 50 U $mL^{-1}$ DNase I (Roche) and 5% FBS for 30 min at 37°C. After being passed through 70-μm mesh sieves, the obtained LPLs were collected by centrifugation at 200 *g* and 4°C for 8 min and analysed via flow cytometry.

## Acquisition of splenic lymphocytes (SPLs) and mesenteric lymph node (MLN) cells

Mesenteric lymph nodes and spleens were removed from sacrificed mice. The fat was stripped, and the tissues were placed in prechilled PBS. The tissues were ground thoroughly on different 70-μm mesh sieves with 3-mL syringe stoppers and washed with PBS. The cells were then separately centrifuged at 140 *g* and 4°C for 5 min and collected into separate centrifuge tubes. The obtained MLN cells were ready for flow cytometry. Erythrocyte lysis buffer was added to splenic cells for 5 min to remove red blood cells; subsequently, the cells were centrifuged to obtain SPLs.

### Cytokine detection assay

Cytokines were detected in the colons of mice in different groups using a mouse Quantibody cytokine array kit (QAM-TH17-1-1, RayBiotech, Norcross, GA, USA) according to the manufacturer's instructions.[64] Three duplicate samples were prepared for each group. An Axon 4000B scanner with GenePix software was used to collect fluorescence intensities. Following background removal and normalisation, each cytokine's concentration in the sample was calculated according to its standard curve. Proteins with significantly different expression levels were identified according to fixed criteria (fold change $\leq 0.83$ or $\geq 1.2$), and GO and KEGG enrichment analyses of the differentially expressed genes were carried out to select key signalling pathways.

### Statistical analysis

Data analysis was performed using a two-tailed unpaired *t*-test or one-way ANOVA with SPSS 20.0 software. $*P < 0.05$ was considered indicative of a significant difference. The data are presented as the mean $\pm$ standard deviation (SD).

## ACKNOWLEDGMENTS

This work was supported by the National Nature Science Foundation of China (81470751 to YL, 81600891 to LG), Beijing Natural Science Foundation (7172087 to YL), Beijing Municipal Administration of Hospitals Clinical Medicine Development of Special Funding Support (ZYLX201703), Beijing Baiqianwan Talents Project (2017A17 to YL), Beijing excellent talent (2014000021469G251 to LG) and Capital Characteristic Clinic Project (Z161100000516203 to LG).

## CONFLICT OF INTEREST

The authors declare no conflict of interest.

## AUTHOR CONTRIBUTIONS

LJ, RW and YL conceptualised the study; LJ, RW, NH, JF, ZL, LG, YS and JD investigated the study; LJ and RW conducted experiments; LJ wrote the manuscript; YL critically revised the manuscript and provided overall supervision. All authors read and approved the final manuscript before publication.

## REFERENCES

1. Maekawa T, Krauss JL, Abe T *et al*. *Porphyromonas gingivalis* manipulates complement and TLR signaling to uncouple bacterial clearance from inflammation and promote dysbiosis. *Cell Host Microbe* 2014; **15**: 768–778.
2. Thapa B, Pak S, Kwon HJ *et al*. Decursinol angelate ameliorates dextran sodium sulfate-induced colitis by modulating type 17 helper T cell responses. *Biomol Ther (Seoul)* 2019; **27**: 466–473.
3. Lin X, Sun Q, Zhou L *et al*. Colonic epithelial mTORC1 promotes ulcerative colitis through COX-2-mediated Th17 responses. *Mucosal Immunol* 2018; **11**: 1663–1673.
4. Shen H, Shi LZ. Metabolic regulation of TH17 cells. *Mol Immunol* 2019; **109**: 81–87.
5. Ouyang W, Kolls JK, Zheng Y. The biological functions of T helper 17 cell effector cytokines in inflammation. *Immunity* 2008; **28**: 454–467.
6. Izcue A, Coombes JL, Powrie F. Regulatory T cells suppress systemic and mucosal immune activation to control intestinal inflammation. *Immunol Rev* 2006; **212**: 256–271.
7. Eastaff-Leung N, Mabarrack N, Barbour A *et al*. Foxp3$^+$ regulatory T cells, Th17 effector cells, and cytokine environment in inflammatory bowel disease. *J Clin Immunol* 2010; **30**: 80–89.
8. Olsen I, Yilmaz O. Modulation of inflammasome activity by *Porphyromonas gingivalis* in periodontitis and associated systemic diseases. *J Oral Microbiol* 2016; **8**: 30385.
9. Martande SS, Pradeep AR, Singh SP *et al*. Periodontal health condition in patients with Alzheimer's disease. *Am J Alzheimers Dis Other Dementias* 2014; **29**: 498–502.
10. Hajishengallis G, Liang S, Payne MA *et al*. Low-abundance biofilm species orchestrates inflammatory periodontal disease through the commensal microbiota and complement. *Cell Host Microbe* 2011; **10**: 497–506.
11. Garlet GP, Martins W Jr, Ferreira BR *et al*. Patterns of chemokines and chemokine receptors expression in different forms of human periodontal disease. *J Periodontal Res* 2003; **38**: 210–217.
12. Matsubara VH, Silva EG, Paula CR *et al*. Treatment with probiotics in experimental oral colonization by Candida albicans in murine model (DBA/2). *Oral Dis* 2012; **18**: 260–264.
13. Kim HW, Hong R, Choi EY *et al*. A probiotic mixture regulates T cell balance and reduces atopic dermatitis symptoms in mice. *Front Microbiol* 2018; **9**: 2414.
14. Matsubara VH, Bandara HM, Ishikawa KH *et al*. The role of probiotic bacteria in managing periodontal disease: a systematic review. *Expert Rev Anti Infect Ther* 2016; **14**: 643–655.
15. Theodoro LH, Claudio MM, Nuernberg MAA *et al*. Effects of *Lactobacillus reuteri* as an adjunct to the treatment of periodontitis in smokers: randomised clinical trial. *Benef Microbes* 2019; **10**: 375–384.
16. Park JS, Joe I, Rhee PD *et al*. A lactic acid bacterium isolated from kimchi ameliorates intestinal inflammation in DSS-induced colitis. *J Microbiol (Seoul, Korea)* 2017; **55**: 304–310.
17. Jia L, Han N, Du J *et al*. Pathogenesis of important virulence factors of *Porphyromonas gingivalis* via toll-like receptors. *Front Cell Infect Microbiol* 2019; **9**: 262.
18. Bron PA, van Baarlen P, Kleerebezem M. Emerging molecular insights into the interaction between probiotics and the host intestinal mucosa. *Nat Rev Microbiol* 2011; **10**: 66–78.
19. Liu G, Zhao Y. Toll-like receptors and immune regulation: their direct and indirect modulation on regulatory CD4$^+$ CD25$^+$ T cells. *Immunology* 2007; **122**: 149–156.

20. Sutmuller RP, den Brok MH, Kramer M *et al*. Toll-like receptor 2 controls expansion and function of regulatory T cells. *J Clin Invest* 2006; **116**: 485–494.
21. Littman DR, Rudensky AY. Th17 and regulatory T cells in mediating and restraining inflammation. *Cell* 2010; **140**: 845–858.
22. Zhou L, Lopes JE, Chong MM *et al*. TGF-β-induced Foxp3 inhibits T(H)17 cell differentiation by antagonizing RORγt function. *Nature* 2008; **453**: 236–240.
23. Eichele DD, Kharbanda KK. Dextran sodium sulfate colitis murine model: An indispensable tool for advancing our understanding of inflammatory bowel diseases pathogenesis. *World J Gastroenterol* 2017; **23**: 6016–6029.
24. Nunes NS, Kim S, Sundby M *et al*. Temporal clinical, proteomic, histological and cellular immune responses of dextran sulfate sodium-induced acute colitis. *World J Gastroenterol* 2018; **24**: 4341–4355.
25. Maloy KJ, Powrie F. Intestinal homeostasis and its breakdown in inflammatory bowel disease. *Nature* 2011; **474**: 298–306.
26. Shale M, Schiering C, Powrie F. $CD4^+$ T-cell subsets in intestinal inflammation. *Immunol Rev* 2013; **252**: 164–182.
27. Trindade SC, Olczak T, Gomes-Filho IS *et al*. *Porphyromonas gingivalis* antigens differently participate in the proliferation and cell death of human PBMC. *Arch Oral Biol* 2012; **57**: 314–320.
28. Carvalho-Filho PC, Trindade SC, Olczak T *et al*. *Porphyromonas gingivalis* HmuY stimulates expression of Bcl-2 and Fas by human $CD3^+$ T cells. *BMC Microbiol* 2013; **13**: 206.
29. Brozovic S, Sahoo R, Barve S *et al*. *Porphyromonas gingivalis* enhances FasL expression via up-regulation of NFkappaB-mediated gene transcription and induces apoptotic cell death in human gingival epithelial cells. *Microbiology* 2006; **152**: 797–806.
30. Yamazaki K, Nakajima T, Ohsawa Y *et al*. Selective expansion of T cells in gingival lesions of patients with chronic inflammatory periodontal disease. *Clin Exp Immunol* 2000; **120**: 154–161.
31. Murali AK, Mehrotra S. Apoptosis - an ubiquitous T cell immunomodulator. *J Clin Cell Immunol* 2011; **S3**: 2.
32. Peluso I, Fina D, Caruso R *et al*. *Lactobacillus paracasei* subsp. *paracasei* B21060 suppresses human T-cell proliferation. *Infect Immun* 2007; **75**: 1730–1737.
33. Kalani M, Hodjati H, Sajedi Khanian M *et al*. *Lactobacillus acidophilus* increases the anti-apoptotic micro RNA-21 and decreases the pro-inflammatory micro RNA-155 in the LPS-treated human endothelial cells. *Probiot Antimicrob Proteins* 2016; **8**: 61–72.
34. Ivanov II, McKenzie BS, Zhou L *et al*. The orphan nuclear receptor RORγt directs the differentiation program of proinflammatory IL-$17^+$ T helper cells. *Cell* 2006; **126**: 1121–1133.
35. Isogai E, Isogai H, Kimura K *et al*. *In vivo* induction of apoptosis and immune responses in mice by administration of lipopolysaccharide from *Porphyromonas gingivalis*. *Infect Immun* 1996; **64**: 1461–1466.
36. Afzali B, Mitchell PJ, Edozie FC *et al*. CD161 expression characterizes a subpopulation of human regulatory T cells that produces IL-17 in a STAT3-dependent manner. *Eur J Immunol* 2013; **43**: 2043–2054.
37. Abbas AK, Benoist C, Bluestone JA *et al*. Regulatory T cells: recommendations to simplify the nomenclature. *Nat Immunol* 2013; **14**: 307–308.
38. Hartigan-O'Connor DJ, Hirao LA, McCune JM *et al*. Th17 cells and regulatory T cells in elite control over HIV and SIV. *Curr Opin HIV AIDS* 2011; **6**: 221–227.
39. Laurence A, Tato CM, Davidson TS *et al*. Interleukin-2 signaling via STAT5 constrains T helper 17 cell generation. *Immunity* 2007; **26**: 371–381.
40. Jung MK, Kwak JE, Shin EC. IL-17A-producing $Foxp3^+$ regulatory T cells and human diseases. *Immune Netw* 2017; **17**: 276–286.
41. Komatsu N, Okamoto K, Sawa S *et al*. Pathogenic conversion of $Foxp3^+$ T cells into TH17 cells in autoimmune arthritis. *Nat Med* 2014; **20**: 62–68.
42. Hoffmann P, Boeld TJ, Eder R *et al*. Loss of FOXP3 expression in natural human $CD4^+CD25^+$ regulatory T cells upon repetitive *in vitro* stimulation. *Eur J Immunol* 2009; **39**: 1088–1097.
43. Hang L, Kumar S, Blum AM *et al*. *Heligmosomoides polygyrus bakeri* infection decreases Smad7 expression in intestinal $CD4^+$ T cells, which allows TGF-β to induce IL-10-producing regulatory T Cells that block colitis. *J Immunol* 2019; **202**: 2473–2481.
44. AlQallaf H, Hamada Y, Blanchard S *et al*. Differential profiles of soluble and cellular toll like receptor (TLR)-2 and 4 in chronic periodontitis. *PLoS One* 2018; **13**: e0200231.
45. Shi G, Vistica BP, Nugent LF *et al*. Differential involvement of Th1 and Th17 in pathogenic autoimmune processes triggered by different TLR ligands. *J Immunol* 2013; **191**: 415–423.
46. Bhaskaran N, Cohen S, Zhang Y *et al*. TLR-2 signaling promotes IL-17A production in $CD4^+CD25^+Foxp3^+$ regulatory cells during oropharyngeal candidiasis. *Pathogens* 2015; **4**: 90–110.
47. Liu H, Komai-Koma M, Xu D *et al*. Toll-like receptor 2 signaling modulates the functions of $CD4^+$ $CD25^+$ regulatory T cells. *Proc Natl Acad Sci USA* 2006; **103**: 7048–7053.
48. Ben-Nun A, Wekerle H, Cohen IR. The rapid isolation of clonable antigen-specific T lymphocyte lines capable of mediating autoimmune encephalomyelitis. *Eur J Immunol* 1981; **11**: 195–199.
49. Haskins K, McDuffie M. Acceleration of diabetes in young NOD mice with a $CD4^+$ islet-specific T cell clone. *Science* 1990; **249**: 1433–1436.
50. Morrissey PJ, Charrier K, Braddy S *et al*. $CD4^+$ T cells that express high levels of CD45RB induce wasting disease when transferred into congenic severe combined immunodeficient mice. Disease development is prevented by cotransfer of purified $CD4^+$ T cells. *J Exp Med* 1993; **178**: 237–244.
51. Izcue A, Hue S, Buonocore S *et al*. Interleukin-23 restrains regulatory T cell activity to drive T cell-dependent colitis. *Immunity* 2008; **28**: 559–570.
52. Seif F, Khoshmirsafa M, Aazami H *et al*. The role of JAK-STAT signaling pathway and its regulators in the fate of T helper cells. *Cell Commun Signal* 2017; **15**: 23.
53. Chen Z, Laurence A, O'Shea JJ. Signal transduction pathways and transcriptional regulation in the control of Th17 differentiation. *Semin Immunol* 2007; **19**: 400–408.

54. Burchill MA, Yang J, Vogtenhuber C *et al*. IL-2 receptor beta-dependent STAT5 activation is required for the development of Foxp3$^{+}$ regulatory T cells. *J Immunol* 2007; **178**: 280–290.
55. Loomer PM, Sigusch B, Sukhu B *et al*. Direct effects of metabolic products and sonicated extracts of *Porphyromonas gingivalis* 2561 on osteogenesis *in vitro*. *Infect Immun* 1994; **62**: 1289–1297.
56. Chen J, Zhao Y, Jiang Y *et al*. Interleukin-33 contributes to the induction of Th9 cells and antitumor efficacy by dectin-1-activated dendritic cells. *Front Immunol* 2018; **9**: 1787.
57. Liu Y, She W, Wang F *et al*. 3, 3′-Diindolylmethane alleviates steatosis and the progression of NASH partly through shifting the imbalance of Treg/Th17 cells to Treg dominance. *Int Immunopharmacol* 2014; **23**: 489–498.
58. Tang J, Xiong J, Wu T *et al*. Aspirin treatment improved mesenchymal stem cell immunomodulatory properties via the 15d-PGJ2/PPARγ/TGF-β1 pathway. *Stem Cells Dev* 2014; **23**: 2093–2103.
59. Zheng B, van Bergenhenegouwen J, Overbeek S *et al*. *Bifidobacterium breve* attenuates murine dextran sodium sulfate-induced colitis and increases regulatory T cell responses. *PLoS One* 2014; **9**: e95441.
60. Park JS, Choi J, Kwon JY *et al*. A probiotic complex, rosavin, zinc, and prebiotics ameliorate intestinal inflammation in an acute colitis mouse model. *J Transl Med* 2018; **16**: 37.
61. Suzuki K, Sun X, Nagata M *et al*. Analysis of intestinal fibrosis in chronic colitis in mice induced by dextran sulfate sodium. *Pathol Int* 2011; **61**: 228–238.
62. Deng J, Liu Y, Yang M *et al*. Leptin exacerbates collagen-induced arthritis via enhancement of Th17 cell response. *Arthritis Rheum* 2012; **64**: 3564–3573.
63. Roselli M, Finamore A, Nuccitelli S *et al*. Prevention of TNBS-induced colitis by different *Lactobacillus* and *Bifidobacterium* strains is associated with an expansion of γδT and regulatory T cells of intestinal intraepithelial lymphocytes. *Inflamm Bowel Dis* 2009; **15**: 1526–1536.
64. Che N, Li X, Zhang L *et al*. Impaired B cell inhibition by lupus bone marrow mesenchymal stem cells is caused by reduced CCL2 expression. *J Immunol* 2014; **193**: 5306–5314.

## Supporting Information

Additional supporting information may be found online in the Supporting Information section at the end of the article.